Modification of Cellulose for Metal Ions Adsorption and Degradation of Organic Pollutants.

Faiza Lughmani

Regn. # 00000172897

A thesis submitted in partial fulfillment of the requirements

for the degree of **Master of Science**

in

Chemistry

Supervised by: Dr. Mudassir Iqbal

Department of Chemistry

School of Natural Sciences

National University of Sciences and Technology

H-12, Islamabad, Pakistan

2019

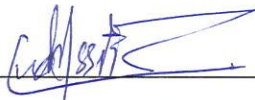# National University of Sciences & Technology

M.Phil THESIS WORK

We hereby recommend that the dissertation prepared under our supervision by: Faiza Lughmani, Regn No. 00000172897 Titled: Modification of Cellulose For Metal Ions Adsorption and Degradation of Organic Pollutants be accepted in partial fulfillment of the requirements for the award of **MS** degree.
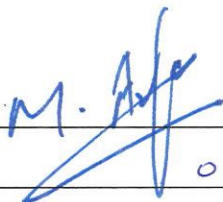
Examination Committee Members

1. Name: DR. MUHAMMAD ARFAN   Signature:

2. Name: DR. SYED RIZWAN HUSSAIN   Signature:

External Examiner: DR. SHAHID ALI   Signature:

Supervisor: DR. MUDASSIR IQBAL   Signature:

_____
Head of Department

07/10/19
Date

COUNTERSINGED

Date: 07/10/19

_____
Dean/Principal

THESIS ACCEPTANCE CERTIFICATE

Certified that final copy of MS thesis written by **Ms. Faiza Lughmani**, (Registration No. **00000172897**), of **School of Natural Sciences** has been vetted by undersigned, found complete in all respects as per NUST statutes/regulations, is free of plagiarism, errors, and mistakes and is accepted as partial fulfillment for award of MS/M.Phil degree. It is further certified that necessary amendments as pointed out by GEC members and external examiner of the scholar have also been incorporated in the said thesis.

Signature: _____

Name of Supervisor: Dr. Mudassir Iqbal _____

Date: _____ 07/10/19

Signature (HoD): _____

Date: _____ 07/10/19

Signature (Dean/Principal): _____

Date: _____ 07/10/2019

Dedication

Dedicated to my Beloved Parents Mr. Muhammad Nazir

Lughmani and Mrs.Shahnaz Begum (late)

Acknowledgements

Abstract

Various types of dyes are widely used in textile industries. Extensive usage of these dyes leads to water contamination. This contaminated water is hazardous for human beings and for other live form as well. Therefore it is necessary to treat the polluted water. These dyes can be removed from water using biodegradation method but this method is really not that efficient. Use of metallic nanoparticles for degradation of dyes provides promising benefits to the environment. In this thesis cellulose was modified to acid and amino functionalized derivatives and employed as supporting material for the synthesis of copper nanoparticles. Copper ions from aqueous solution was adsorbed on films of prepared derivatives and then treated with sodium borohydride solution in order to synthesize zero valent copper nanoparticles. Immediate change in color depicts the formation of nanoparticles which was also confirmed by XRD analysis. The prepared derivatives of cellulose were characterized using FT-IR and CHNS analysis. UV-VIS spectroscopy was performed for the degradation studies of dyes. Results revealed that all the films showed degradation only in the presence of ZVC nanoparticles. Oxidized cellulose and MCC-Hyd and MCC-DEM showed excellent degradation efficiencies i.e. more than 85% in all cases. Reason behind is functionalization provides more adsorption sites for metals ions ultimately leads to formation of larger amount of nanoparticles. While for pure cellulose degradation efficiency was low because of less adsorption of copper ions from aqueous solution.

Contents

List of Abbreviations

MCC	**Microcrystalline cellulose**
DMAC	N,N Dimethyl acetamide
LiCl	Lithium chloride
OC	Oxidized cellulose
NC	Nanocellulose
p-TsCl	Para toluene sulfonylchloride
AUG	Anhydroglucose unit
TsMCC	Tosylated microcrystalline cellulose
RT	Room temperature
L	Liter
FT-IR	Fourier transformed infrared spectroscopy
XRD	X-ray diffraction
SEM	Scanning electron microscopy
TGA	Thermo gravimetric analysis
AAS	Atomic absorption spectroscopy
ICP-OES	Inductively coupled plasma optically emission spectrometry
EDX	Energy dispersive X-rays spectroscopy
UV-VIS	Ultra-violet visible spectroscopy
CNC	Cellulose nanocrystals
CO	Carbon monoxide
CFC's	Chloroflouro carbons
HM	Heavy metals
NPs	Nanoparticles
ZVC	Zerovalent copper
CNF	Cellulose nanofibers
ChNF	Chitosan nanofibers
CMC	Carboxymethyl cellulose

CA	Cellulose acetate
EDTA	Ethylenediaminetetraacetic acid
DTPA	Diethylenetriaminepentaacetic acid
MO	Methyl orange
MB	Methylene blue
CR	Congo red
4-NP	4 Nitrophenol
Cu	copper
CH-FP	Chitosan coated filter paper
CH-CC	Chitosan coated cotton cloth
TEA	Triethyl amine
D.I	Deionized water
Cu^0-MCC	Zerovalent copper nanoparticles embedded microcrystalline cellulose
Cell-hyd	6-Deoxycellulose hydrazide
Cell-DEM	6-Deoxycellulose (N,N-diethyl)amine

LIST OF FIGURES

List of Tables

Chapter 1

Introduction

Our environment is continually evolving but as environment is changing so does the problems related to it. With uncertain weather patterns, influx in natural disasters and much more it is very important to be aware of all these problems and their consequences. Pollution is amongst the one of the major problems our Earth is experiencing now a day.

1.1 Pollution

Presence of any substance or its induction into the environment causing poisonous or harmful effects is called as pollution.

Air, water and soil are polluted by chemical compounds and their bi-products. Agricultural and industrial wastes pollute the water that is harmful for human, plants and animals. Different human activities like deforestation, mining, littering and construction deteriorate the earth's surface causing land pollution. Hazardous smoke from industries, traffic, burning of fossil fuels and tanneries directly pollutes the air.

1.2 Environmental Pollution

Environmental pollution basically refers to the three major environmental components i.e. air, water and soil. They may account to acute or chronic harm to the ecosystem. Pollutants may be chemical in nature and their results could also be harmful physical phenomena i.e. greenhouse gases leading to global warming [1] [2]. Pollution is being caused when the natural environment is unable to degrade an element or substance without generating destruction to itself. The elements involved are not produced by nature, and the destroying process can vary from a few days to thousands of years (that is, for instance, the case for radioactive pollutants). In other words, pollution takes place when nature does not know how to decompose an element that has been brought to it in an unnatural way[3].

Environmental pollution has existed for centuries but only started to be significant following the industrial revolution in the 19th century [4], it must be taken seriously, as it has a negative effect on natural elements that are an absolute need for life to exist on earth, such as water and air. Indeed, without it, or if they were present in different quantities, animals including humans and plants could not survive. Pollution is mainly caused due to the careless use of fossil fuels and not properly dumping of industrial waste.

1.3 Types of Pollution

Five main forms of pollution are as follow:

- ➢ Soil pollution
- ➢ Air pollution
- ➢ Water pollution
- ➢ Noise pollution
- ➢ Light pollution

1.4 Soil pollution

Soil pollution is the degradation of soil because of human or natural activities. Soil has direct contact with life on earth so its contamination also risks health. Various chemicals like polynuclear aromatic hydrocarbons, lead, heavy metals, organic solvents, pesticides and dyes are main causes of human main soil pollution. These chemicals are most common cause of pollution because they are very persistent and generally accumulate in the subsoil layer[5].

1.5 Water pollution

The importance of water in our lives can be understand from the fact that no living being can survive on earth without water. Marine water covers the extensive part of water on the earth which is not fit for drinking purposes without proper processing. The only source of drinking water is fresh water from water bodies and from underground water. The quality of water is extremely essential in our life as physiological activities of biological cells depend mainly on water. Water comprises 2/3 of our body and we cannot survive without water even for one day. The human brain contains 95% water[6]. A reduction of even 2% water content in body can cause dehydration.

Water is required by all cells and organs of living organisms for the maintenance of their physiology and anatomy [7].

Water contamination is the addition of harmful contents to the water as it doesn't remain fit anymore for the drinking purposes as well for the survival of aquatic and marine life[8]. Water contamination is dangerous not only for marine life but also a big danger to whole ecosystem. Water pollution has now become a major problem for global system as it is increasing day by day and it causes numerous fatal deaths. Not only industrial waste caused the water pollution but some natural phenomena like earth quakes, storms, land sliding etc., contributing towards the lowering of water quality. There are different causes of water pollution and addition of these toxins to the water and harming the lives.

Recent studies show that agricultural lands have very large amount of phosphorous (P) and nitrogen (N) transported through streams and river pathways [5]. Pakistan stands at 80 among 122 nations in world drinking water problems ranking [9]. In Pakistan over 16 million people are unable to approach clean water drinking for. 250,000 children decease every year because of water borne diseases.

1.6 Sources of water pollution

A report published by Environment Protection Agency (EPA) in 1990 which showed that more than 50% of the water contamination of water bodies is produced by the leaching of chemical from landfills where they are used to increase crop production[9].

Sources of water pollution can be of two main types. Point sources which comes from single and identifiable source like domestic sewage, industrial effluents and mining etc. Other one is non - point source or sometimes attributed as diffuse pollution in which we cannot define single source e.g. agricultural land in which fertilizers, animal manure, pesticides and soil washed into streams as a result of rainfall are all non-point sources [10]. Sources of water contamination can be in form of physical or chemical pollutants like change in temperature, large objects that are visual, dyes that change color of water or pesticides that are colorless but cause hazardous effects on human and marine life. Literature have shown that in USA the amount of Fertilizers using nitrogen and phosphorous in their contents are increased 20-fold from 1945-1993 [11] and nitrogen is main

source of pollution. In Asia major source of water pollution are organic matter, heavy metals, deforestation, eutrophication and pathogens [12].
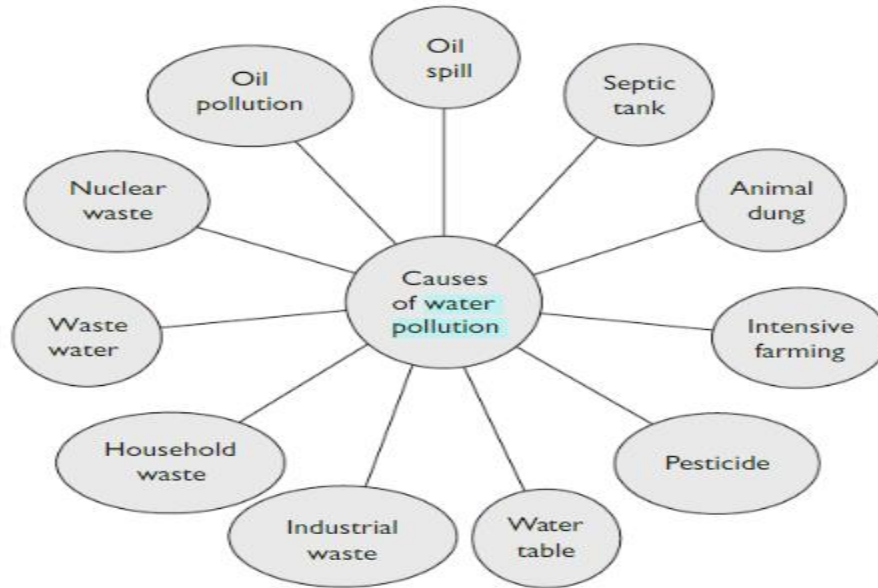
Figure 1.1 Major causes of water pollution.

1.7 Pollutants and Their Effect on Human Health

Pollution is a severe menace to the human health.[10, 11]. Due to water pollution, many diseases are arising like diarrhea, cholera malaria dengue[10], typhoid, HIV/AIDS. Air pollution also has many severe effects on human health as many hazardous gases like carbon dioxide CO_2 carbon oxide CO, sulfur oxides and CFC's are released into environment unchecked[12]. Asthma, lungs cancer[13], TB and other breathing problems are arising due to air pollution. Land pollution is also caused due to the high usage of fertilizers, pesticides, herbicides, and dumping of untreated non-degradable materials like radioactive elements. Industrial waste containing textile dyes, paints, and other detergents when released unprocessed causes many serious health issues like cancer, kidney, liver and skin diseases.

1.8 Heavy metals
The word "heavy metal" (HM) covers those elements whose specific gravity is five times greater than that of water like lead, arsenic, cadmium and mercury[14]. Among 35 metals which are of

ecological concern, 23 of them represent heavy metals. Chromium, arsenic, mercury, lead and cadmium are rated among 20 most harmful substances as per ATSDR / US EPA[15].

The release of wastewater from industries containing heavy metals is one of the most sensitive ecological issues worldwide [16]. Industrial wastes that carry heavy metal contaminants usually present in water are lead (pb), chromium (Cr), cadmium (Cd), copper(Cu) and arsenic (As) [17, 18]. Due to increased rigorous protocols and laws, HM are treated as priority pollutants. Presence of such poisonous metals in wastewater pose a great threat to the humans as well as environment. Consequently, their extraction from wastewater should be carried out with low cost and ecofriendly adsorbents [19].

Removal of HM is the need of hour as it results in serious health issues which include disorders of central nervous system (CNS), organ damage, diminutive growth and development, cancer and sometimes even death [20]. Heavy metals like lead and mercury in wastewater may lead to the phenomena of autoimmunity by which immune system destroys itself on its own [21]. Besides, this may result in multiple diseases like malfunction in nervous system, fetal brain, circulatory system, kidney diseases and rheumatoid arthritis [22]. Heavy metals in excessive amounts may cause permanent damage to brain.

Wastewater usually contains heavy metals in dilute quantities (1 - 100 mg/L) and at neutral (pH = 7.0) or acidic pH values (pH < 7.0) and are generally considered to be those whose density exceeds 5 g per cubic centimeter[23]. Their removal from the wastewater was done in many techniques depending upon the type of heavy metal and its concentration.

The release of heavy metals into aquatic environments has become a severe trouble over the past few decades. As a result of various industrial processes these pollutants are introduced into the marine ecosystems. The chemically contaminated water has severely damage the ecology of surface and groundwater; ultimately having serious concerns on life form in polluted area. Electroplating, textile, Tanning, metallurgical waste and mining and are the most significant causes of ecological pollution by heavy metals. In Pakistan, there are 670 textile entities that are discharging their wastes material into water streams without waste management [24]

Copper is one of the substantial toxic heavy metal found in waste discharge and not decomposable, travels through the food chain. Although presence of copper (Cu) in trace amounts serves a vital role in humans to maintain sound health [25, 26]. Nevertheless, its uptake beyond nominal concentration may be hazardous. Copper contamination in water may come from electrical factories. It may cause vomiting, convulsions, diarrhea, muscular cramps and atrophy. MCL value for Cu as per USEPA and WHO is 1.3 mg/L and 1.0 mg/L respectively[15, 27]

1.9 Dyes

Dyes are sort of pigments which are used to color different substances but mostly used on fibers and leather made products. Dyes are aromatic organic compounds and have affinity for the particular substances. Most of the dyes are used in the form of aqueous solutions.

The solubility of dyes in water is because of the auxochromes i.e. -OH, -Cl, -Br, -NO2, - COOH, -NHR, -NH2 etc. Auxochromes have the ability to ionize in water thus making dyes soluble and these groups are also responsible to intensify colors of dyes.

Auxochromes can be classified based on their charge and nature i.e. acidic or basic [28].

1.9.1   Color of dyes
Dyes are organic aromatic compounds but they pose colors [29] because:

> ➢ They absorb light in visible region.
> ➢ They have color bearing groups (chromophores).
> ➢ They exhibit resonance of electrons.
> ➢ They have a conjugated system.

1.9.2   Types of dyes

Mainly dyes are classified as:

a) Natural dyes

b) Synthetic dyes

Animals and plants are the sources of natural dyes. Like Tyrin purple and madder are natural dyes extracted from sea snails and madder root respectively. Synthetic dyes are classified as azo dyes and non-azo dyes. Azo dyes are further classified as acidic, basic and reactive, disperse and Sulfur dyes [19]. Synthetic dyes can also be classified as acidic and basic based on their nature. Figure 1.8 shows the flow chart for the classification of dyes.
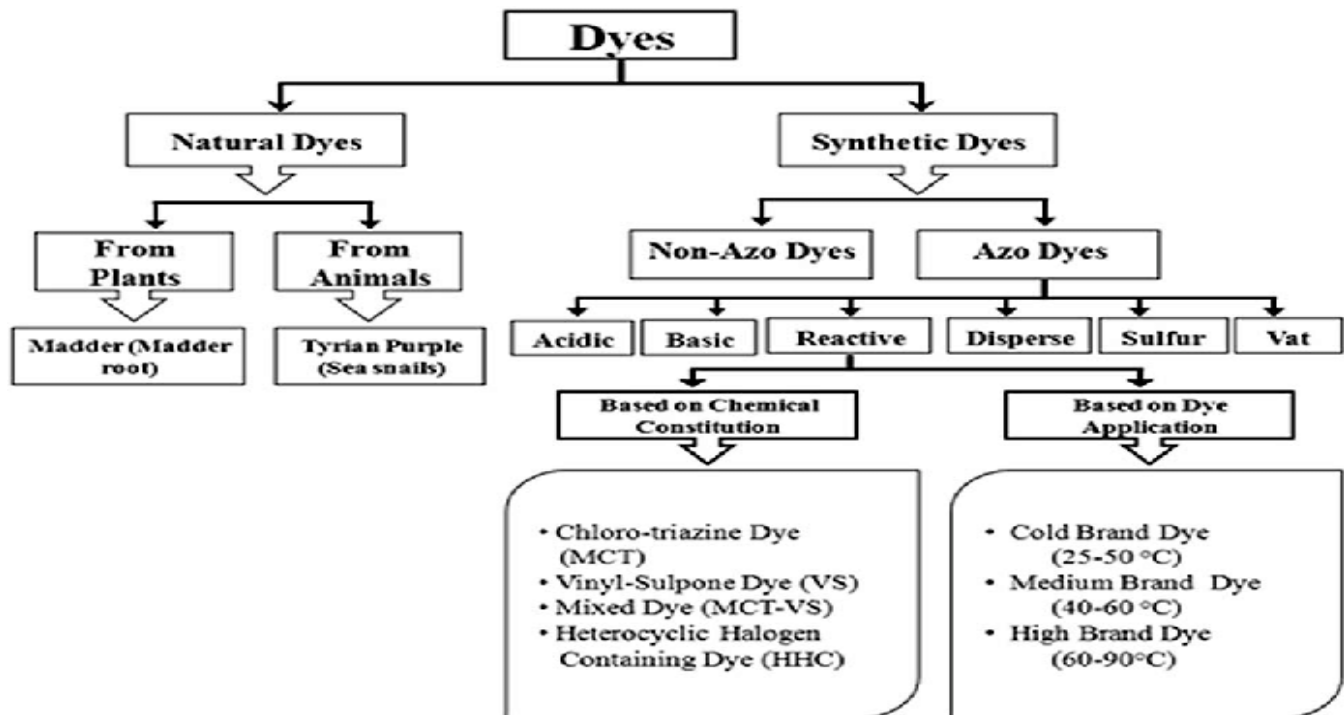
Figure 1.2. Classification of Dyes.

Among all available dyes, mostly dyes are azo dyes. These dyes are used in different industries like pharmaceuticals, textile and cosmetics. Dyes are quite toxic as well so improper discharge of waste water having dyes leads to serious skin and respiratory problems.

1.9.3 Uses of dyes

Dyes are mainly used in laboratories as indicator, ink printing and textile industry.

Textile Industry:

Till 19th century only natural dyes were used as textile dyes, but later on synthetic dyes are being used in textile industry. After then, synthetic dyes are being extensively used due to their advantages like easy production and availability of dyes in different colors. The discharge of these dyes in water leads to its contamination when released untreated in water bodies. These synthetic dyes in waste water are highly carcinogenic due to the presence of harmful organic compounds like naphthalene and benzidine.

Printing Ink:

Different heavy metal are used as pigments in printing industry including titanium oxide, aluminum and brass. Leaching of these heavy metals in water causing its contaminations leading to serious health issues.

Many health hazards are caused by these dyes including;

1. When these dyes enter into water they can absorb and reflect light which can directly affect the process of photosynthesis in alga leading to the disturbance of food chains of many lives.
2. The existence of even minute quantity of dyes in water can affect the purity and transparency of water to a greater extent which damages aquatic environment.
3. Mostly dyes are carcinogenic and a big danger to life.
4. Textile Dyes can cause many allergic reactions in eyes, skin diseases and respiratory problems.
5. Dyes can cause the cancer of kidney, urinary bladder and liver in people working with these dyes continuously.

1.10 Strategies of Dye Degradation

Effluents from industries containing dyes products has serious effect on color and quality of water. It also affects the health of human beings as well as aquatic life. So it is highly mandatory to

remove these dyes and pesticides from the waste water to avoid serious consequences. Following methods are being employed for the degradation of water contaminants.

1. Physical methods.
2. Biological methods
3. Chemical methods.

1.11   Need of Dye Degradation

Although dyes have many benefits but they are also dangerous to human life in many different ways. Following are the several hazards of dyes [30]

- Dyes are most of the times soluble in water and thus they cause pollution in water. This water when discharged in to rivers, it causes severe damage to aquatic as well as human life.
- Dyes affect the absorption and reflection of sunlight from water thus affects the underwater photosynthetic activity.
- A lot of dyes are carcinogenic and some can cause irritation to skin.
- Transparency of water bodies are greatly affected by the small amount of dyes which are even undetectable by human eye. So, these harmful dyes need to be removed or better, degraded for the survival of living beings.

Therefore, an effective strategies are required for the treatment of diminution of organic waste in order to eradicate, or at least minimize the amount of toxic substances from waste water. Various techniques are being employed to eliminated colored chemicals and hazardous metals, are electrochemical treatment, filtration, precipitation, osmosis, flotation, coagulation, flocculation and adsorption.[31-36] The major hindrance in attaining the success of physical methods is the limitation associated with, such as expense, the possibility of secondary pollutants formation, and partial treatment, hence there is need to focus on the development of methods that completely transformed   organic pollutants, especially with the assist of an efficient catalyst.

1.12 Metallic Nanoparticles

Due to their applications in various areas, metallic nanoparticles have drawn growing attention in recent years. These includes[37].

➢ Sensing
➢ Drug delivery
➢ Bio-imaging
➢ Antibacterial coating

Metallic nanoparticles considered as widely employed catalyst for the degradation of organic pollutants; because of large surface area, catalytic efficiency, easy production and selectivity for particular type of reactions. They were used in different reactions involving coupling reactions, electrochemical reactions, and oxidation and reduction reactions [38].

However, the low stability of most abundantly available metal nanoparticles restricts the actual environmental applications in contrast to noble metals which exhibit more stable nanoparticles. For example, copper nanoparticles are highly susceptible to air and under ordinary circumstances are quickly oxidized, which may restrict their practical applications. In the same conditions, nickel nanoparticles also tend to be unstable in the air [39-41]. Other problems associated with use of nanoparticles are agglomeration and separation. Because of extremely small size it's very difficult to separate nps from reaction mixture. Agglomeration occurs as a result of van der Waals interactions, it causes reduction of surface area and hence decreases catalytic efficiency[42].

1.13 Why cellulose??

➢ Natural
➢ Most abundant biopolymer
➢ Environment benign
➢ Cost effective
➢ Non-toxic
➢ Biodegradable
➢ Biocompatible

Chapter 2

Literature survey

This chapter involved all the literature that was reviewed before and during this research work. There are a lot of research has been done on cellulose based biosorbents, synthesis of ZVC and theirutalization in reduction of organic azo dyes. This thesis includes some of the literature already done on synthesis of zero-valent copper nanoparticles, modification of cellulose, various biosorbents and their usage for adsorption of metal ions and use of use of ZVC for catalytic degradation of different types of organic dyes.

2.1 Nanocellulose as biosorbents.

Peng Liu et. al. (2015) uses enzymatic phosphorylation to enhance the adsorption efficiency of various type of nanocellulose composites. Characterization techniques used were FTIR spectroscopy, AFM and zeta seizer to study the molecular structure, morphology and surface potential of prepared derivatives of nanocellulose. In order to measure the amount of heavy metal ions ICP-OES was used. Selectivity of heavy metals capacity to adsorb (Fe^{+3}, Cu^{+2}, and Ag^{+2} was investigated in industrial discharge as well as in model water. Both modified and unmodified nanocellulose show potential for immobilization of Cu^{+2}, Fe^{+3} and Ag^{+2}. Studies revealed that sulphonate, carbonyl and phosphate groups are responsible for the biosorption of metal ions. In aqueous solution 100% immobilization of Cu^{+2}, Ag^{+2}, and Fe^{+3} has been observed with phos-CNC_{BE} and phos-CNF_{SL}.in solutions that contains single type of metal ions, the high surface selectivity order was Ag^{+2}, Cu^{+2}, Fe^{+3}, while the order changed to Ag^{+2}, Fe^{+3}, Cu^{+2} for solution containing mixture of ions. 99% removal efficiency of heavy metals ions (Fe^{+3} and Cu^{+2}) was observed from industrial waste that has been taken from mirror industry.[43]

Xiaolin yu et al. (2013) reported nonoabsorbent for the Pb^{+2} and Cd^{+2} from aq. solution. Succinic anhydride was used to synthesized SCNCs; it was then treated with NaHCO3 to obtain sodic nanoabsorbent (NaSCNCs). The synthesized SCNCs and NaSCNCs were verified by characterization like FTIR and NMR. Prepared SCNCs and NaSCNCs were used for the

elimination of Pb^{+2} and Cd^{+2}. Adsorption was checked with batch adsorption isotherm was checked with batch adsorption experiment. Results show that adsorption rate was faster with NaSCNCs. Various factors i.e. effect of pH, concentration, contact time, regeneration performance and coexisting ions were studied. It was noticed that adsorption of metal ions (Pb^{+2}, Cd^{+2}) increase with the increase of pH. Pb^{+2} adsorption is higher with NaSCNCs then SCNCs. Langmuir model confirmed the adsorption isotherms.465.1 mg/g, 344.8 mg/g and 367.6 mg/g, 259.7mg/g are the highest adsorption capabilities for cd^{+2} and pb^{+2} of SCNCs and NaSCNCs. Saturated solution of NaCl was used for the regeneration of NaSCNCs.[44]

2.2 Modified cellulose as biosorbents:

Houssine et al. (2014) used surface chemical modification to increase the adsorption capacity of microcrystalline cellulose and chitin fibers for heavy metal ions. Characterization tools employed were UV visible spectroscopy, wavelength dispersive X-rays, scanning electron microscopy, X-ray photoelectron spectroscopy, FTIR and elemental analysis. Metal ions studies were Cu^{+2}, Cr^{+2},Ni^{+2},and Zn^{+2}.Chitin nanofibers and cellulose nanofibers had relatively a less functionalities on their surface which results in low adsorption of copper ions (13mg/g for CNF while 27mg/g for ChNF). Oxidation treatment enhances the adsorption capacity of copper for both the nanofibers. Carboxylate ions provide negative sites for the electrostatic attraction of Cu+2 ions. The increased metals ions adsorption is associated directly to the solution pH, and amount of carboxylate ions present. The maximum adsorption value of cu+2 for highly oxidized cellulose is 135mg/g and 55mg/g is for chitin nanofibers. The adsorption capacities of other ions (Cr^{+2}, Zn^{+2} and Ni^{+2}) were also investigated. Adsorbed metal ions can easily be desorbed from contaminated fibers through acidic washing and can be reused.[45]

Shani peng et al. (2014) prepared nanoporous magnetic cellulose-chitosan composite microsphers using sol gel transition method for Cu (II) sorption. Ionic liquids were used as solvents. Composites microspheres were characterized by SEM, foriour transformed infra-red FTIR, TGA, XRD and VSM.. Results revealed that presence of chelating groups, NMCMS exhibited efficient adsorption amount of Cu^{+2}. Langmuir isotherm best describe the Cu^{+2} adsorption of composite microspheres. Kinetic of adsorption data describes the pseudo-second order kinetics. HCl was used for the

regeneration of adsorbed NMCMS and they can be used upto five times, thus proving to be cheap and eco-friendly.[46]

I.M Kenawy et al. (2018) synthesized guanyl modified cellulose (Gu-MC) for the elimination of metal ions (Zn^{+2}, Pb^{+2}, Hg^{+2}, Cd^{+2}, Cu^{+2}) from aq. solution. SEM, TGA and FTIR were used for the characterization of prepared material. Effects of different factors on adsorption capacities of metal ions were studied. As the temperature increases the adsorption of metal ions decreased with because of less interaction between active sites (imino C=NH and C=N groups) of Gu-MC and metal ions. Results depicted that adsorption capacity of Gu-MC increased by increasing the metal ions concentration. The highest adsorption values were 83, 78, 68, 52, and 48 mg/g for Cu^{+2}, Zn^{+2}, Cd^{+2}, Pb^{+2}, and Hg^{+2} respectively. Results showed second order kinetic model, which revealed chemical adsorption as rate limiting step.[47]

Cuinua Dong et al. (2016) prepared sulfonated cellulose for the efficient abstraction of HM ions. The modified cellulose was analyzed by TGA, XRD, FT-IR Spectroscopy and zeta potential analyzer. Reduction in crystallinity of sulfonated cellulose was observed in XRD, which shows release of OH groups and destruction of crystallinity. Results illustrates that adsorption of sulfonated cellulose was highly dependent on temperature, amount of metal ions & loading of absorbent. Metal ions uptake efficiency for Fe^{+3}, Cu+2 and Pb+2 were 98.7%, 47.5% and 83.0% respectively. The removal efficiency of Fe+3 reduced slightly in the presence of Pb+2 and Cu+2 from 98.7% to 84.6% and 87.2% respectively. However, efficiency of copper and lead lessened to 13.3% and 17.2% respectively. Order of adsorption efficiency for all the three ions was Fe+3>Pb+2>Cu+2. Showing Fe+3 can efficiently be separated from Pb+2 & Cu+2 by sulfonated cellulose. For desorption of metal ions EDTA was used as chelating agent along with 0.1M HNO3 or HCL. Slight decrease in zeta potential value occurred after adsorption of metal ions to sulfonated cellulose. Adsorption equilibrium reached within 2min, which shows fast and excellent adsorption.[48]

Repo et al. (2010) successfully synthesized EDTA and DTPA grafted composites and characterized them by FTIR, XRD, FESEM, and TGA. Prepared composites were used for the uptake of Co^{+2} & Ni^{+2} ions. Adsorption of co^{+2} and Ni^{+2} by EDTA-Chitosan composite was found to be 63.0mg/g and 71.0mg/g respectively while with DTPA-Chitosan composite it was 49.1 and

53.1 mg/g correspondingly. At pH value of 2.1 and 2g/L of adsorbent concentration the efficiency of reached from 93.6% to 99.5%.[49]

R. Saravanan et al. (2015) used sodium metaperiodate for oxidation of cellulose, which was then condensed with p-toluidine. Modified cellulose contain methyl benzalaniline group which acts as antibacterial as well as chelating agent for heavy metal ions. Characterization techniques used were FT-IR, SEM, TGA, EDX, ^{13}C-MAS. Batch experiment was accomplished at different pH, adsorbent concentration, time and various metal ion concentrations. SEM images showed irregular open porous & rough surface of modified cellulose. Particle size was observed to be 448.3nm. EDX spectra showed additional peaks of Pb+2 & Cu+2 after adsorption. More than 70% of metal ions adsorption occurred at lower ph value. Optimum dose of adsorbent was 20mg. maximum adsorption of DTD for Cu+2 was 157.3 mg/g and 153.5 mg/g for P+2. Langmuir isotherm model better described experimental results. Adsorption process was pseudo-second order and exothermic reaction.[50]

Sun et al. (2009) processed chitosan/cellulose composites for adsorption of HM ions copper (Cu (II), zinc Zn(II), chromium Cr(VI), nickel Ni(II) and lead Pb(II)). Ionic liquid was used as a solvent. The adsorption capacity for Cu(II) was 26.5 mg/g, 19.81 mg/g for Zn(II), 13.05 mg/g for Cr(VI), 13.21 mg/g for Ni(II) and 26.31 MG/G for Pb(II). Langmuir isotherm model well describe the results obtained.[51]

Sazlinda et al. (2017) prepared cellulose acetate membrane (CAM) using casting method. These were then used for the efficient elimination of copper (Cu) and cadmium (Cd) ions. FESEM, BET, and FTIR analysis was used for the conformation of CAM formation. Flame atomic adsorption spectroscopy was used for the quantitative and qualitative analysis of metal ions. The adsorption capacities were examined at parameters like adsorbent concentration, ph, desorption, kinetic parameters, prescien and reusability. Water samples were taken from different sources i.e. river, sea water and drinking water. The optimum pH was found to be 8 and 10 with 0.035g and 0.012g of adsorbent concentration for cu^{+2} and cd^{+2} ions respectively. Moreover the extreme adsorption capability was found to be 14.21 mg/g and 11.20 mg/g for Cu^{+2} and Cd^{+2} respectively. Pseudo-second order kinetics and rate constant 0.66 mg/g and 1.75 mg/g for copper ions and cadmium

ions was observed. 32.06% and 44.21% are the highest percentages of desorption of metals. CAM can be used efficiently up to three cycles without changing the adsorption capacity.[52]

Nuri Astrini et al. (2015) successfully synthesized poly (acrylic acid)/monmorilionite grafted carboxymethyl cellulose composites abbreviated as CMC-g-PAA/MT. These prepared composites were used for adsorption of heavy metals. Batch experiment was carried out. Composite formation wasverified by FTIR and SEM analysis which also shown that complex formation between metal ions and carboxyl groups of composite was responsible for adsorption. Atomic adsorption spectroscopy (AAS) was used to measure the initial and final concentration of Pb^{+2} and Zn^{+2} in solution. The optimal pH was establish to be 5 with adsorption capacity 286.67 mg/g and 146.19 mg/g for Zn^{+2} and Pb^{+2} respectively. For desorption 0.1mol/L (HNO_3) nitric acid and 0.1mol/L sodium hydroxide (NaOH) are used. These also acts as regenerating agents.[53]

Min Xiao et al. (2017) used EDA/KSCN 70/30 (w/w) solvent system to prepare cellulose/chitosan composite. Methanol was used as coagulating agent. Adsorption of cadmium Cd^{+2}, copper Cu^{+2}, and lead Pb^{+2} onto the composite surface was investigated. It was observed that metal concentration is directly prportional to the adsorption. At pH 5 maximum uptake of metal ion was noticed. At initial concentration of 200mg/L the composite (1:1) absorbed 0.28mmol/g Cd+2, 0.016mmol/g Pb^{+2} and 0.053mmol/g Cu^{+2}. WAXD analysis shows that crystallinity of both cellulose and chitosan was reduced in composite thus increasing amorphous polymer. XPS studies revealed that N-atoms of composite were involved in interaction with metal ions releasing its lone pair of electrons. It was also confirmed that composite was stable in aqueous acidic solution. Freundlich model best describe adsorption isotherms and kinetics was found to be second order. Reusability of adsorbent is up to three cycles with minor decrease in adsorption capacity.[54]

Nan Li et al. (2005) prepared chitosan-cellulose hydrogel absorbent for the efficient eridication of Cu^{+2} ions from aq. solution. EGDE was used as crosslinking agent, which also improves the chemical stability of absorbent in acidic medium. Characterization techniques used were FTIR, SEM, Zeta potential measurement, XPS. SEM revealed the spherical morphology with mean diameter of 3.1mm. FTIR results showed that after crosslinking amine peak shifted and becomes weaker as soon as adsorption of Cu^{+2} ions occurred, indicate N-atoms to be the chief adsorption

sites for Cu^{+2} on hydrogel beads. This was also confirmed by XPS analysis. For cross-linked beads freundlich model was used while for cellulose-chitosan composite Langmuir model was well fitted with data obtained. Highest adsorption occurred at neutral pH.[55]

Genlin zhang et al. 2014 modified carboxymethyl cellulose with acrylic acid. The prepared derivative was used for the degradation of methyl orange (MO), disperse blue, malachite green. Modified cellulose derivative was characterized using FTIT and SEM analysis. Batch adsorption studies were performed and various parameters (PH, time, temperature) were investigated. 84.2% of methyl orange was degraded at ph value of <4.0 at 65°C while at ph value of 7and 7, temperature 45°C and 40°C, 79.6% and 99.6% of degradation was observed for disperse blue and malachite green chloride in about 40min. Temkin isotherm well explained the equilibrium of reaction while k inetics was found to be pseudo-second order.[56]

E. M. Bakhsh et. al. (2011) prepare cellulose acetate based composites. Fabrication of CA was done by incorporation of ferric-oxide nanoparticles via a physical blending of solution. CA/Fe_2O_3 was used as support for Cu, Ag and Nickel nanoparticles and evaluated for reduction studies of 4-NP and MO. Reaction describes the pseudo-first order kinetic and rate constant for MO and 4-NP was $4.77\times10^{-3}\,s^{-1}$ and $8.58\times10^{-3}\,s^{-1}$ respectively. Silver nps on CA/Fe_2O_3 reveled excellent catalytic performance for MO and 4-NP. And it can be reused upto 6 time with little reduction in efficiency.[57]

2.3 Plants based modified Adsorbents:

Futao wang et al. (2017) prepared sugarcane cellulose based bioadsorbent in order to eradicate Pb^{+2}, cu^{+2}, and $zinc^{+2}$ ions from aq. solution. The effect of temperature and metal ions concentration was inspected. The obtained biosorbent was characterized with XRD, SEM, and FTIR for morphological and structural analysis. Langmuir isotherm model was in accordance with the adsorption of zinc Zn^{+2}, copper Cu^{+2} and lead Pb^{+2}. The highest values of adsorption capacities in a single component system were, 363.3mg/g, 446.2mg/g and 558.9 mg/g respectively. For the better description of binary component the competitive Langmuir model was used. In this system the 3D sorption surface described that efficiency of copper ions decreased in the presence of Pb+2

ions, while there is no effect on efficiency of other metal ions. The motivating force behind the adsorption process is the coordination between ions and biosorbent, ion exchange and electrostatic interactions [58]

Etim at al. (2012) used coconut coir dust without any physical or chemical modification for the adsorption of methylene blue (MB) from aqueous solution. Results showed nonlinear relation adsorption and pH but linear increased in adsorption was observed with time, adsorbent concentration and temperature. Kinetics parameters and adsorption isotherms (Freundlich, Langmuir & temkin) were also investigated. Kinetics was observed to be pseudo-second order. Adsorption of MB with coconut coir dust was exothermic in nature and change in enthalpy (ΔH) was +17.87 kj/mol. It was suggested that adsorption was via a chemical interactions of functional groups.[59]

Sentruk et al. (2010) presented almond shells as biosorbent. It was evaluated for the adsorption of Rhodamine 6G in batch experiment at various parameters. Both Langmuir and freundlich well describe the experimental results. Monolayer biosorption was absorbed in Langmuir model. Kinetics of biosorption at all concentrations of dyes was pseudo-second order. Adsorption capacity was 32.6mg/g and process was spontaneous and endothermic.[60]

M. Boumediene et al. (2014) inspected the abstraction of MB dye by using cellulosic wastes namely almond peel and orange peel. FTIR, SEM, TGA, Biochemical and elemental analysis were performed to characterize the biosorbent. Adsorption isotherms and kinetics of adsorption was studied at various initial concentrations and contact time. For understanding of mechanism of biosorption adsorption models were analyzed with experimental data. $\Delta G°$, $\Delta H°$, and $\Delta S°$ of the reaction were calculated in thermodynamic studies. Batch experiment was carried out at 400rpm agitation and temperature $25°C \pm 1°C$ with 1gm of adsorbent and 1L solution of dye (MB). Equilibrium was achieved in 18min with 2.5×10^{-5} mg/L of initial dye concentration. Results showed that increasing concentration of dye decreased the adsorption process, reason behind were agglomeration. Kinetics was first order Langmuir isotherm revealed adsorption capacities to be 208.8 mg/g for almond while 218.82 mg/g for orange peel. $\Delta S°$ values were 75.32 J/mol/K and 47.34 J/mol/K, $\Delta H°$ 14.816 kj/mol and 7.048 kj/mol for orange and almond peels respectively.[61]

Anna Witek-krowiak et al. (2011) studied metal ions uptake at various parameters (temperature, pH, contact time, absorbent dosage) using peanut shells as an absorbent. Peanut shells was washed, dried, crushed and milled. The obtained particles were less than 30µm in size. Concentrations of Cu^{+2} and Cr^{+2} were determined by AAS. 23.3 mg/g and 27.86 mg/g was found to be the highest adsorption capacity at 20°C, pH 5 and 10 g/L of absorbent concentration. According to kinetic studies equilibrium was achieved in 20min and process was pseudo-second order model.[62]

B. Nasernejad et al. (2005) used carrot residue for metal ions (Cu^{+2}, Zn^{+2}, Cr^{+2}) uptake. Adsorption equilibrium of metal ions has been studied by frundlich and Langmuir isotherms. 75-80% Biosorption occurred within 10min while equilibrium was attained after 1 hour 10min. frundlich isotherm best described the experimental data. From results biosorption capacity was noticed to be in order $Cu^{+2} > Zn^{+2} > Cr^{+2}$.[63]

Hajeeth, t et al. (2013) Uses ceric ammonium nitrate (initiator) to extract cellulose from sisal fibers, and used for the Ni^{+2} and cu^{+2} ions adsorption at various parameters (adsorbent conc., PH, temperature, contact time). The results obtained revealed that the uptake of metal ions is directly relative to the shaking time, pH and concentration of absorbent. The maximum contact time for Ni^{+2} and cu^{+2} ions were 240 and 200 minutes respectively. The maximum concentration of absorbent and optimal pH of media was witnessed to be PH 5 and 4gm. The acquired results shows that the Freundlich model was the appropriate model for the adsorption studies of Ni^{+2} and cu^{+2} ions. Acrylonitrile copolymer grafted cellulose was observed to be the excellent absorbent for uptake of copper and nickel ions under optimum conditions. Adsorption of both copper and nickel obeys pseudo second order kinetics.[64]

2.4 Amino functionalized cellulose based adsorbents.

Cunzhi Zhang et al. (2017) synthesized amino functionalized cellulose and characterized by FTIR, SEM, XPS and TGA. Carboxylated micro crystalline cellulose was prepared by using succinic anhydride and DMF as solvent.it was then used to graft hydroxyl group with PEI to prepare adsorbent PEI/SA-MCC$_{MV}$. The quantity amino and carboxyl group was found to be 2.61

mmol/g and 4.64 mmol/g respectively. The time for Cd^{+2} was 20min and for Pb^{+2} it was 45min. freundlich isother model was well fitted with the PEI/SA-MCC adsorption. Kinetic studies shown pseudo second order reaction. Chelating process was confirmed to be the main adsorption mechanism.[65]

Xitong sun et al. (2014) synthesized amino modified magnetic nanocomposite of cellulose, which involves formation of magnetic silica nanoparticles by co-precipitation method, coating with cellulose then grafting with glycidal methacrylate. At the end reacted with ethylene diamine to get amino modified composites. The prepared composite was verified by FTIR, XRD, TEM, VSM and zeta potential analyzer. Batch experiment was carried out to examine the Cr(VI) ions uptake efficiency. Results concluded that adsorption highly depends upon pH of the solution. Langmuir model showed the maximum adsorption capacity of 171.4 mg/g at pH value of 2 at 25°C. Thermodynamic studies revealed the ions uptake process to be spontaneous in nature and exothermic as well. Equilibrium reached within 10min which showed adsorption to be a rapid process. 0.1mol/L NaOH was used to desorb the metal ions. The Composite revealed a good reusability.[66]

Lijuan et al. 2013 modified cellulose by inducing quaternary ammonium group onto the surface of cellulose for the uptake of reactive red 228 dye. Cellulose was extracted from flax slive. Various parameters were considered to investigate the adsorption. Maximum uptake capacity was observed to be 190mg/g at ph 3 at 20°C for solution of $80mgL^{-1}$ in 6hrs. Langmuir isotherm showed adsorption of R.R228 on adsorbent as chemisorption process. kinetics was pseudo-second order and reaction was exothermic in nature.[67]

S.Sitva et al. 2013 performed modification of cellulose with aminoethanethiol without solvent. Cellulose was first chlorinated with thionyl chloride followed by the treatment with aminoethane thiol in the presence of Et3N as a base. FT-IR, 13CNMR, XRD, TGA and elemental (CHNS) analysis was used to characterize the prepared material. Induction of aminothiol on to the surface of cellulose was confirmed by 13CNMR. Loss of crystallinity was observed in XRD. The best adsorption activity was at pH 2 and 9 with equilibrium time 100 and 160 min respectively.

Langmuir model show adsorption activity of 78mg/g and 25mg/g at pH 2 and 9 respectively while kinetics was pseudo-second order.[68]

S. Silva et al. (2018) used diethylenetriamine to modify cellulose. Cellulose was first treated with phthalic anhydride to get PhCell, it was then treated with diethylenetriamine. The prepared material was employed for the elimination of eosin and methyl orange dye from aqueous media. Characterization tools used were FTIR spectroscopy, DRX, TG/DTG, elemental analysis and 13C-NMR spectroscopy. Elemental analysis revealed the nitrogen incorporation upto 5.55 ± 0.02 mmol per gram of prepared material. FTIR confirmed the presence of (N-H) amide stretch and (C-N) deformation at 3400cm^{-1} and 1330cm^{-1} respectively. Batch experiment showed best adsorption with 25ml solution of EY & MO and 20mg of substrate. At ph value of 4 and equilibrium time about 60min, MO adsorption was 2.9 and 65.45mg/g for cellulose and detecell respectively. While Ey dye took about 140min at Ph 5 and adsorption capacity was observed to be 1.30 and 56.69mg/g in cellulose and detecell respectively.[69]

2.5 Miscellaneous adsorbents:

E.S. Dragon et al. (2014) prepared chitosan modified with polyvinyl (amine) absorbent and used for copper Cu (II) adsorption from aq. solution. FTIR spectroscopy was used to characterize the prepared composite. The maximum uptake efficiency was noticed to be 192.57 mg/g at 25°C and contact time 24hrs. Results revealed that increasing pH value from 2 to 4.5 the uptake capacity of copper ions increased, while it decreased with further rise in pH up to 5.5. The optimum pH value was 4.5. Kinetic studies showed pseudo-second order model.[70]

X. Li. Et al. (2015) successfully synthesized Cs/Go-SH composites. The prepared composites were used for the uptake of Cd(II), Cu(II), and Pb(II). Characterization techniques used were SEM, XRD, TGA, FTIR and Raman spectroscopy. The metal uptake was investigated at several considerations such as pH, contact time, adsorbent amount, and temperature. Metal uptake process was endothermic in nature. According to Langmuir model metal uptake capacity in case of Pb^{+2} was 447 mg/g, for Cu^{+2} 425 mg/g and in case of Pb^{+2} it was 117 mg/g at pH 2.[71]

N.A Negam et al. (2015) prepared glycine-chitosan composite and characterized by FTIR spectroscopy and used for the adsorption of Co^{+2} and Cu^{+2} ions. The maximum adsorption was observed at pH value of 9 and 25C. The optimum contact time was 100min. Langmuir isotherm model best describe the experimental data, while kinetics was pseudo-second order. The composite efficiency for heavy metal removal was 94.1% for Co^{+2} and 95.4% for Cu^{+2}.[72]

Wan ngah et al. (2013) synthesized various composites of chitosan-zeolite namely CZ-0, CZ-1, CZ-2 to adsorb copper ions from aqueous solution. Prepared composites were verified by FT-IR, TGA, SEM, XRD, EDX, pore size, surface area and CHN analysis. Before the uptake of copper ions on CZ composites SEM images showed irregular & plate like surface. While after adsorption agglomeration has been observed at the surface. XRD revealed that crystallinity of zeolites's structure has been destroyed during the composite formation. Batch adsorption studies were carried out at various factors (i.e. pH, quantity of adsorbent etc.). Pseudo-second order kinetics well describes the experimental results. According to Langmuir model, the adsorption capacities of CZ-0, CZ-1, and CZ-2 were found to be 25.61, 51.32, and 14.75mg/g.[73]

Mohammad Ali et al. (2018) synthesized modified chitosan with CDTA and grapheme oxide to gat (Cs/CDTA/GO) nanocomposite. Glutaraldehyde was used as crosslinking agent. Using prepared composites batch adsorption studies were carried out to study various adsorption parameters. The characterization tools used were FT-IR and SEM analysis. The highest adsorption value of nanocomposite adsorbent was 166.98 mg/g with 2g/l adsorbent concentration at pH 3.5. Equilibrium time was 60min. Reaction kinetic was pseudo-second order and all the results was in accordance with Langmuir isotherm. Removal efficiency was found to be 95%. Adsorbent can be reused by simply washing it with 0.1% H_2SO_4 and several times with DI water.[74]

2.6 Zero-valent copper nanoparticles for dye degradation:

Sajjad haider et al. (2016) coated chitosan on cellulose microfibers mat, which acts as substrate for copper nanoparticles synthesis. Copper sulphate solution was used for the uptake of Cu+2 ions on prepared composited. It was then treated with 0.1M NaBH4 solution to obtain Cu^0 nanoparticles. The characterization techniques used were FT-IR, FE-SEM and XRD analysis. The prepared catalyst was employed for the reduction studies of 4-NP, 2NP and cresyl blue dye. XRD

showed crystallite size of Cu^0 nanoparticles to be 48nm.Uv visible spectrophotometer was used to study catalytic reduction of dyes. Roughness of surface was observed in SEM images, which indicated the presence of nanoparticles. EDX analysis revealed weight %age of C, O and Cu to be 40.27, 46.27 and 13.45 % respectively. Degradation of 2-Np & 4-Np followed pseudo-first order and rate constant was observed to be 1.2×10^{-3} S^{-1} and 2.1×10^{-3} S^{-1} respectively while for CB it was $1.3 \times 10^{-3} S^{-1}$. Catalyst can be reused.[75]

Pan Li and coworkers (2015) used zero-valent copper (ZVC) nanoparticles with hydrodynamic cavitation for the degradation of methyl orange dye. Effect of pH, discharge pressure and concentration of nanoparticles on degradation was investigated. ZVC nanoparticles were analyzed using SEM, EDX and particle size analyzer. MO degradation was studied by copper nanoparticles with and without hydrodynamic cavitation. Presence of HC enhanced the degradation efficiency of the reaction. At lower pH of solution, decolorization of MO was more favorable. Reaction kinetics was found to be pseudo-first order and rate constant increases with raise in dose of copper nps. Apparent reduction in size of Cu nanoparticles was observed after HC.[76]

Nauman Ali et al. (2018) successfully synthesize copper nanoparticles for reduction of toxic dyes. Chitosan coated cotton cloth was used as a substrate. Characterization techniques SEM, EDX, XRD and TGA were used to characterize the prepared nanoparticles. Average size of particle was noticed to be 80 and 90nm. The reduction of toxic azo-dyes was investigated in the presence of NaBH4 solution. Cu/Chi-CC was used as catalyst. Catalytic experiment was performed in the glass cuvette in UV-Visible spectrophotometer. Results showed that by increasing the amount of Cu nanoparticles, the pollutant dye degrade rapidly. During degradation process catalyst show brilliant stability and recyclability, as it remain active up to three cycles.[77]

Muhammad Ismail et. al. (2018) used Durantia erecta extract for the synthesis of Cu nanoparticles. The extract behave as capping as well as reducing agent. Analytical techniques used for the characterization were FE-SEM, EDX, TGA, and XRD. Copper nanoparticles as catalyst showed excellent catalytic activity. 96% reduction of methyl orange occurs in 4min while it takes 5min for CR to reduce up to 90.35%. FE-SEM images showed spherical shaped Cu NPs with no aggregation. DEX analysis revealed sharp signals of copper and %age weight of Cu was

found to be 50.50%. An absorption peak at 588nm was observed in UV visible spectrum of copper nanoparticles. Reaction kinetics was pseudo-first order with rate constant $5.07 \times 10^{-3} S^{-1}$ and $8.6 \times 10^{-3} S^{-1}$ for CR & MO respectively[37]

Tahseen et al. (2016) used filter paper as cellulose support having high surface area. Chitosan was coated over cellulose microfibers of filter paper. Copper nanoparticles were synthesized in chitosan layers. 0.1M copper sulphate hexahydrate solution was used for the Cu+2 adsorption. 0.8M NaBH4 solution was used for the reduction of cu+2 to Cu0 nanoparticles. SEM, FT-IR, XRD, analysis were employed for the verification of prepared samples. NaBH4 alone in the presence of CH-FP cannot reduce methyl orange. 100% degradation was observed in the presence of Cu/CH-FP within 13min, while for it takes 17 min to degrade.[42]

Tahseen et al. (2016) synthesized titanium oxide nanoparticles coated chitosan composites and cellulose microfiber mat and were checked for the reduction of thymol violet. Techniques used for the analysis of prepared composites were XRD, FT-IR, SEM and EDX. Adsorption studies were investigated at various parameters like solution's pH, adsorbent quantity and time. Results showed that composites that were pre-treated with solution of higher pH exhibit greater adsorption capacities. Reaction kinetics was noticed to be pseudo-second order and equilibrium was attained in 90min. 97.51 mg/g and 84.32mg/g were maximum uptake efficiency for TiO2/Cs-CMM and Cs-CMM respectively.[78]

Fayaz Ali et al. (2017) used rapid and ecological method for the production of metal nanoparticles on chitosan coated over cotton cloth. Chitosan was coated over strips of cotton cloth using 2wt% chitosan solution. Metal ions (Fe^{+2}, Co^{+2}, Cu^{+2}, Ni^{+2}) were adsorbed on CH-CC strips by keeping the strips in aqueous solutions of respective salts for 2 hrs. Followed by the reduction of metal ions by 0.1M NaBH4 solution to M°. Prepared catalyst was employed for the reduction of 4-NP, degradation of MB, MO and Rh-B. M°/CC-CH strips were characterized by using ATR-FTIR, TGA, FE-SEM, XRD & XPS techniques. For catalytic reduction studies UV visible spectroscopy was used. The prepared ZV Nps exhibited excellent catalytic activity for dyes reduction and conversion of 4-NP to 4-AP. Among these catalysts Fe°/CC-CH strips showed greater activity with rate constant of 0.3804 min^{-1}, 0.2937 min^{-1}, 0.1698 min^{-1} and 0.2802 min^{-1} for Rh-B, 4-NP,

MO, and MB respectively. Strips can easily be recovered from reaction mixture and can be reprocessed several times with little reduction in efficiency.[79]

S.A Khan et. al. (2019) prepared cellulose acetate based heterostructure nanocomposite, which acts as support material for zero-valent copper, silver and for bimetallic CuAg nanoparticles. ZnO was prepared via a sol-gel method it was then then embedded on cellulose acetate polymer. The prepared catalyst was used for the reduction of azo dyes and nitroarenes. Prepared material was characterized by using FT-IR, FESEM, EDS and XRD analysis. ICP-OES was used to check the metal ions uptake efficiency. UV-VIS spectroscopy was used to evaluate the degradation studies of dyes. Results showed that increasing amount of ZnO/CB to the cellulose acetate polymer enhances the catalytic efficiency. Bimetallic CuAg/ZCA 5wt% showed excellent catalytic performance. Rate of reduction was highest for Congo red dye, reason might be the presence of more number of N-atoms in the structure as compared to other dyes. [80]

Chitosan and MCM based various nanocomposites were prepared by **S.A Khan et. al. (2016)** prepared materials were used for the elimination of both anionic and cationic species from water bodies. Silica being charged at surface can easily attracts dyes from wastewater. FT-IR, XRD, FESEM AND EDS analysis were employed for characterization of prepared materials. Dyes used were acridine orange, congo red, indigo carmine and methyl orange. No results has been observed for acridine orange with all the nanocomposites while good adsorption has been observed for all other dyes.[81]

Aim of work.

This thesis describes an effort to modify cellulose for the adsorption of metal ions. The aim was to make a polymer support for the preparation of Cu^0 nanoparticles. And its implementation as catalyst for efficient degradation of Congo red, methyl orange, methylene blue and 4-NP.

Following are the detailed objectives of the study.

- ➢ Chemical modification of cellulose.
- ➢ Preparation of cellulose and modified cellulose film.
- ➢ Using cellulose and derivatized cellulose films for adsorption of metal ions.
- ➢ Synthesis of zero-valent copper nanoparticles by chemical reduction method.
- ➢ Using cellulose as support material for the synthesis of ZVC nanoparticles.
- ➢ Performing degradation studies with all the prepared films.

Chapter 3

Experimental section

This chapter covers the details of the chemicals and experimental procedure employed in this work.

3.1 Chemicals:

Microcrystalline cellulose (MCC), Nitric acid, Phosphoric acid, Sodium nitrite, Sulphuric acid, Sodium hydroxide, para Toluene sulfonyl chloride, Lithium chloride anhydrous, Triethyl amine, Copper Sulphate, Sodium borohydride, Ninhydrin

3.2 Solvents:

Acetone, N, N-Dimethyl acetamide (DMAc), ethanol, N, N-Dimethyl formamide (DMF), chloroform, D.I water.

All chemicals used for the synthesis and preparation of desired catalysts and composites are of high purity and no further purification was needed.

3.3 Instrumentation:

Analytical balanceATY22d was used to weigh accurately all chemicals. FTIT-ATR model ALPHA 200d88 was used to check the reaction progress and identification of functional groups of synthesized compounds. CHNS analysis was performed for elements detection. SEM and XRD analysis was used for conformation of nanoparticles. UV-VIS spectrophotometer was used for the reduction studies of the dyes.

3.4 Synthesis of Cellulose Derivatives:

3.4.1 Preparation of Oxidized Cellulose (OC):

Oxidized cellulose was synthesized by using acidic mixture and $NaNO_2$ as oxidizing agent. Mixture of Nitric acid and phosphoric acid were taken in 4:1 (v/v). To 70ml solution of the acidic mixture, 5.0g of MCC was added. Sodium nitrite ($NaNO_2$) 1.0g was added simultaneously. An instantaneous creation of reddish brown fumes occurred. To inhibit the discharge of fumes to the open air, the reaction flask was enclosed with a petri dish. At room temperature reaction was continued for 48hrs with occasional stirring. After 48 hrs. The mixture seemed green in color. An excess of distilled water was added to reaction mixture. The green color terminated and white fluffy solid was acquired. This mixture was filtered and washed several times with distilled water till the pH of filtrate become 4. Solid obtained was finally washed with acetone and dried. [82, 83].
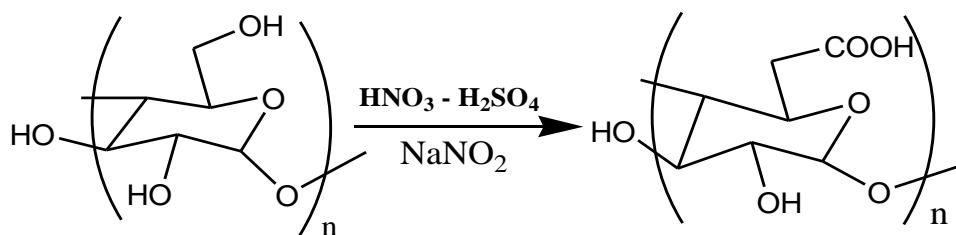
Figure 3.1 synthesis scheme of oxidation of cellulose.

3.4.2 Tosylation of Microcrystalline Cellulose:

Tosylation of cellulose has been performed in two steps.

**Step I: dissolution of cellulose:**

Microcrystalline cellulose was kept in vacuum oven for drying at 70°C. Then 120ml of DMAC was added to the MCC (5.0g, 30.8mmol of anhydroglucose unit) in 500ml round bottom flask (Rb), and stirred at 120-130°C for two hrs. It was then cooled to 100°C and 10g anhydrous LiCl in 25ml f DMAc were added under stirring. The stirring was sustained overnight until complete

dissolutionof cellulose. A transparent gel like solution formed which indicates complete dissolution.

Step II: Tosylation of cellulose:

A mixture of TEA (18.6ml, 185mmol, 6 mol/AGU) in 10ml DMA was added to the gel like solution of MCC under energetic stirring at RT, the stirring was sustained for another 30min, followed by the drop wise addition of p-toulenesulfonyl chloride (35.3g, 184.8mmol, 6mol/AGU) (dissolved in 25ml of DMA) over a period of 30-6-min at 3-8°C. The stirring was continued for another 24hrs at R.T. then the mixture was poured slowly in 1L of ethanol. Precipitation occurs, the precipitate was filtered off, and washed carefully with approximately 1L of distilled water. Again washed with ethanol (250ml) for three times in order to remove unreacted TsCl. The resulted TsMCC was kept in an oven at 50°C for 48hrs for drying [84, 85].
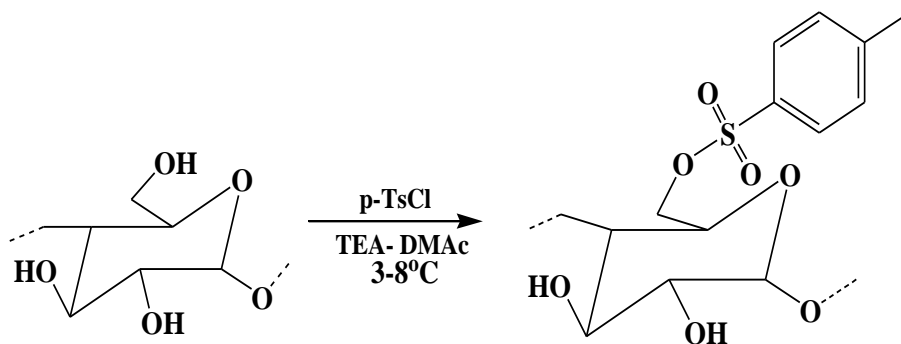
Figure 3.2. Synthesis scheme of Tosylation of Cellulose.

3.4.3 Synthesis of Amino Cellulose:

6-Deoxycellulose hydrazide (MCC-Hyd):

2g of TsMCC was mixed with 20ml of DMF in 100ml round bottom flask at room temperature. The reaction mixture was allowed to react under stirring until the complete dissolution. Then addition of 10ml hydrazine hydrate was done under stirring. At room temperature the stirring was continued for another 2hrs and then the reaction mixture was refluxed at 80°C for 24hrs. Orange color solution was obtained. This mixture was allowed to cool down and then poured slowly into

250ml of ethanol, formation of white precipitates occurred. This was then filtered and washed with ethanol thrice. Dried at 50°C under vacuum for 24hrs.

6-Deoxycellulose (N, N-diethyL) Amine (MCC-DEM):

2g of TsMCC was mixed with 20ml of DMF in 100ml round bottom flask at room temperature. The reaction mixture was allowed to stir until the complete dissolution. Then 10ml of diethyl amine was added under stirring. The stirring was continued for another 2hrs and then the reaction mixture was refluxed at 80°C for 24hrs. Orange color solution was obtained. This for 24hrs reaction mixture was allowed to cool down and then poured slowly into 250ml of ethanol, formation of white precipitates occurred. This was then filtered and washed with ethanol thrice. Precipitates obtained were kept in oven at 50°C for drying.
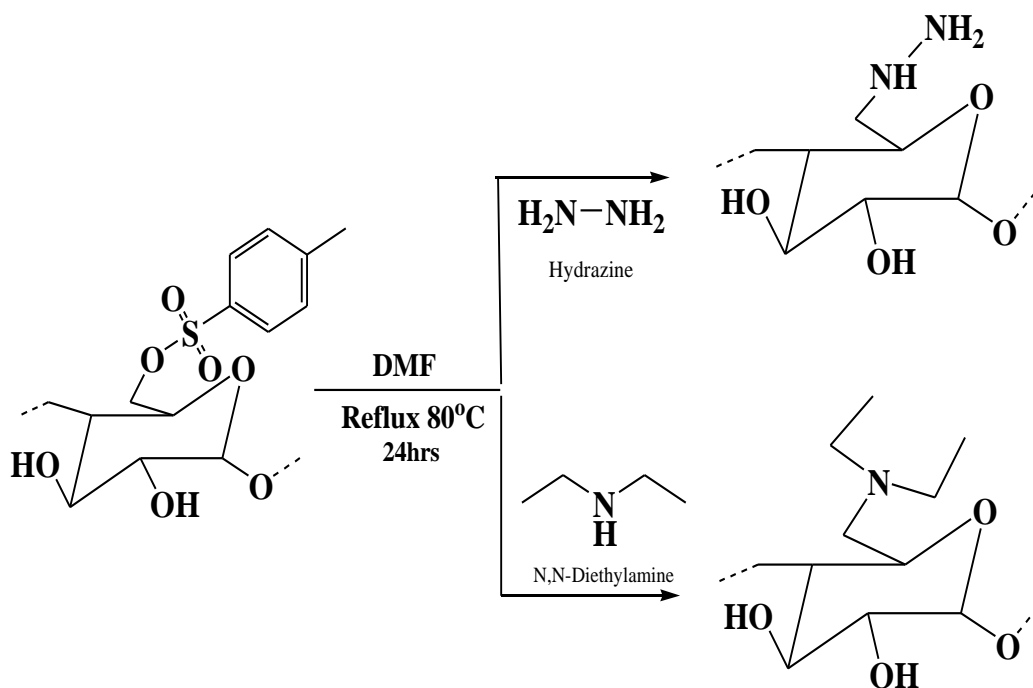

Figure 3.3. Synthesis scheme of cellulose amine derivatives.

3.5 Catalyst Preparation

3.5.1 Preparation of cellulose and modified cellulose films

Composite films of cellulose and modified cellulose were prepared by mechanical mixing. SIS-polymer was used as a binding agent in order to strengthen the films. 0.1g SIS was dissolved in

20ml of chloroform under continuous stirring at room temperature. 1g Cellulose was dispersed in this mixture, stirring was continued for 1hr. after the complete dispersion the mixture was poured into petri dishes and left overnight for evaporation. Dried films were then peeled off and used further. Films of oxidized cellulose, amino-cellulose, and their composites were made by this method.

3.5.2 Preparation of copper nanoparticles

Copper nanoparticles were synthesized inside the layers of polymer films by uptake of Cu^{+2} ions followed by their reduction. Prepared films were dipped in 100ml of 1M $CuSO_4.7H_2O$ solution for adsorption of Cu^{+2} ions. Films were left in copper sulphate solution of 24hrs for saturation of adsorption sites. After adsorption films were washed with D.I water and then kept in 50ml of 0.5M $NaBH_4$ solution in order to reduce Cu^{+2} ions to Cu^0 nanoparticles. After that (Cu^0-MCC) Films were washed gently with deionized water and used freshly.

3.6 Catalytic Reduction Studies:

The catalytic reduction studies were evaluated in the 4-nitrophenol and various azo dyes (Congo red, methylene blue, methyl orange, methyl violet) reductions using sodium borohydride. Quartz cuvette cell was used as reaction container. Solutions of 4-NP, dyes and sodium borohydride were prepared in D.I water with concentrations of 0.5Mm, 0.08Mm and 0.5M respectively. 3ml of 0.08Mm 4-Nitrophenol was taken in a cuvette cell to which 0.5ml of 0.5M freshly prepared $NaBH_4$ solution was added and its spectra on UV visible spectrophotometer was recorded. After that, Cu°/Ch-MCC strips were placed in this cuvette cell in such a position that UV light can easily pass through it. Reduction reaction was started as soon as the catalyst strips were placed in reaction vessel (cuvette) and absorption spectra was continuously recorded. The variations in absorbance value at 400nm for 4-nitrophenol was plotted and compared with calibration curve. For the reduction of other dyes (CR, MB, MO) same procedure was employed.

Chapter 4

Results and Discussions.

This chapter includes all the characterization techniques performed and all the results concluded from different studies.

4.1 Fourier Transformed Infrared spectroscopy (FT-IR).

FTIR is used to attain information about functional groups present in substances. Organic compounds and some inorganic compounds absorb electromagnetic radiations of IR region $4000cm^{-1}$ to $400cm^{-1}$($2.5\mu m$ to $25\mu m$) and produce stretching and bending vibrations by transition of electrons in same electronic shell from lower vibrational level to higher vibrational level. Variable dipole moment of bonds is responsible for vibrations that appear in the form of IR spectra.[86]


Figure 4.1 FT-IR Spectrophotometer.

4.1.1 FT-IR Spectra of MCC, OC and TsMCC.

The FT-IR examination of MCC shows following absorption bands, a broad absorption band at 3325.55 cm^{-1} for –OH stretching. –OH bending was observed at 1372.61cm^{-1} while –CH bending was at 1236.73 cm^{-1} .epoxy stretching at 1024 cm^{-1} corresponds to glycosidic linkage in the structure of cellulose.

Figure 4.2 illustrates the FT-IR spectrum of microcrystalline cellulose.
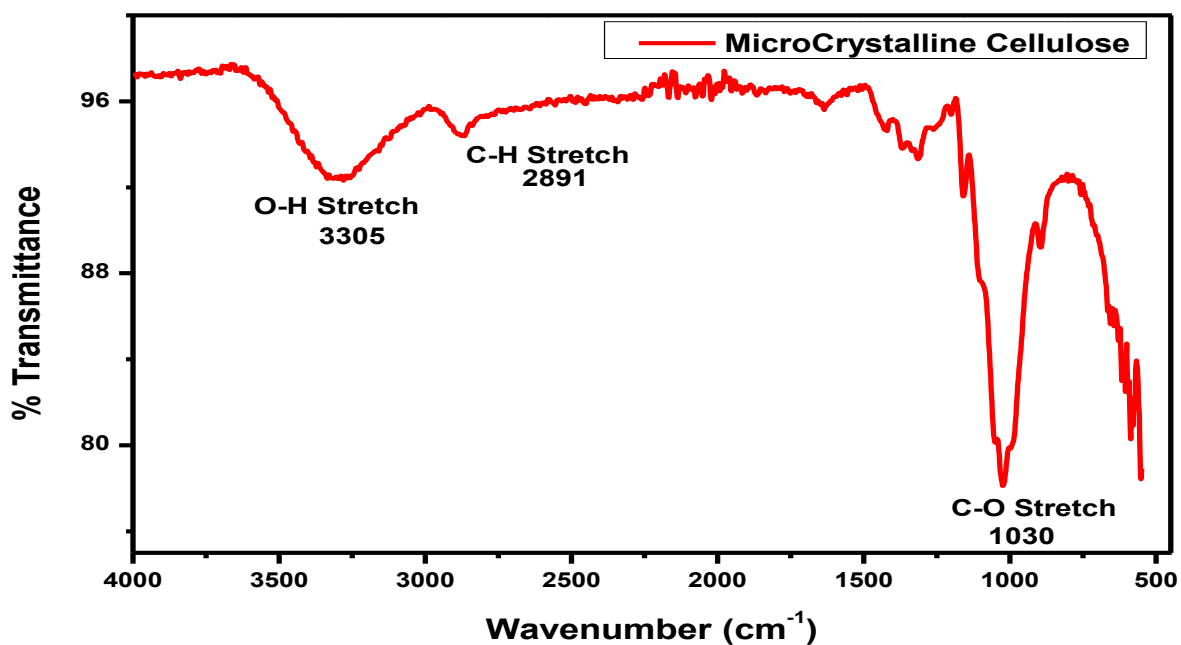
Figure 4.2 Spectrum of microcrystalline cellulose for FT-IR analysis.

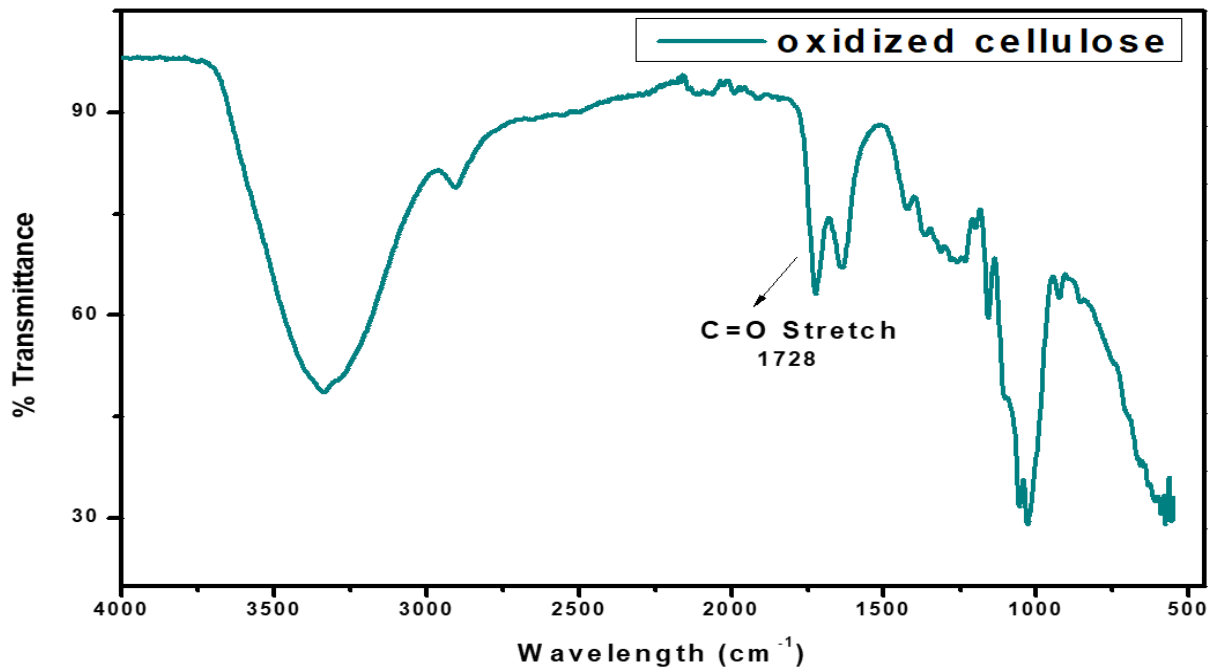Figure 4.3 shows the IR spectrum of oxidized cellulose.

Figure 4.3 FT-IR of oxidized cellulose (OC).

A strong absorption band at 1728 cm^{-1} corresponds to the presence of carbonyl stretching, confirms the presence of acidic group (oxidation).

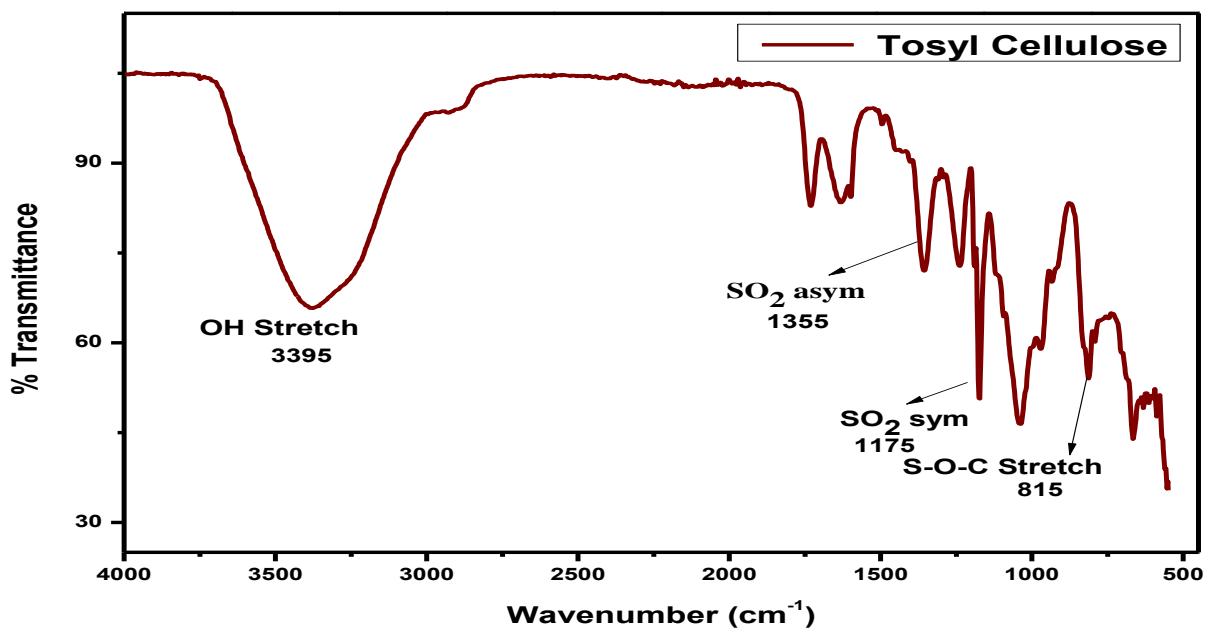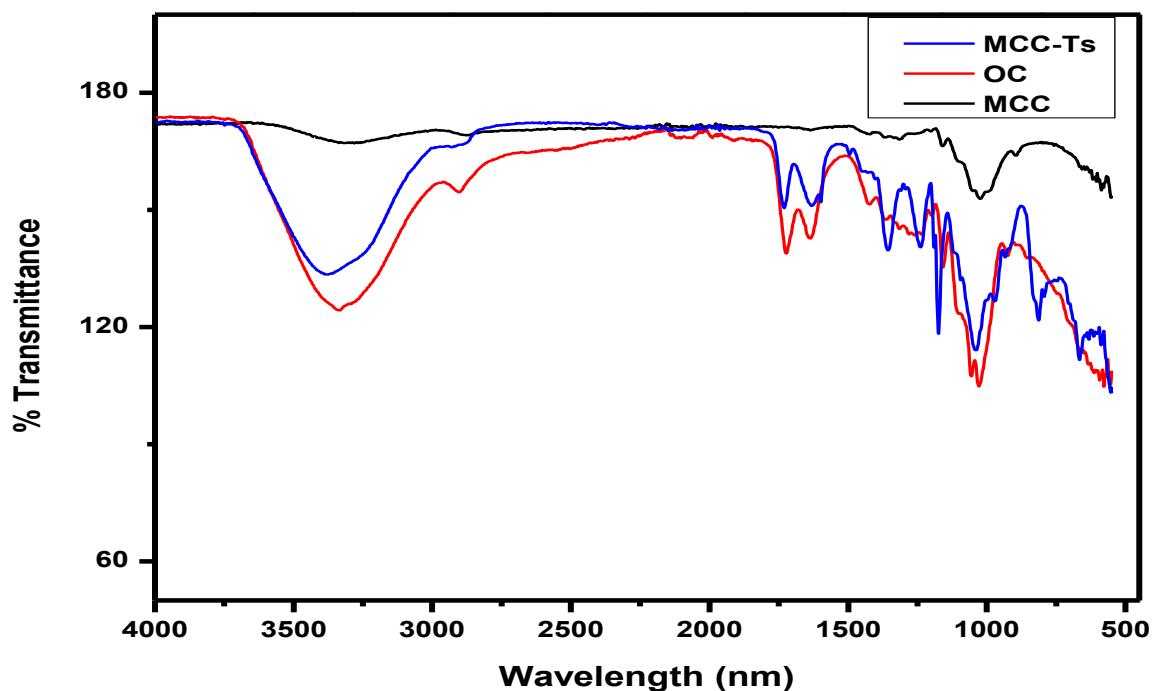*Figure 4.4 FT-IR of Tosylated cellulose.*

FT-IR analysis of tosylated cellulose is shown in figure 4.4. Spectrum shows additional peaks of –SO_2 asymmetric stretch at 1355 cm^{-1}. A band of –SO_2 symmetric stretch is observed at 1175 cm^{-1}. At 815 cm^{-1} the band observed corresponds to –S-O-C stretching vibrations.

Figure 4.5 Superimposed FT-IR Spectra.

4.1.2 FT-IR Analysis of Amino functionalized cellulose:

Tosyled cellulose has been reacted with hydrazine in the presence of DMF as a solvent. Tosyl group has been replaced by hydrazide group. Figure 4.6 shows the FT-IR analysis of cell-Hyd. The additional bands appeared in the spectrum justifies that surface is functionalized with hydrazine hydrate. And the values for their absorption band are given in figure.
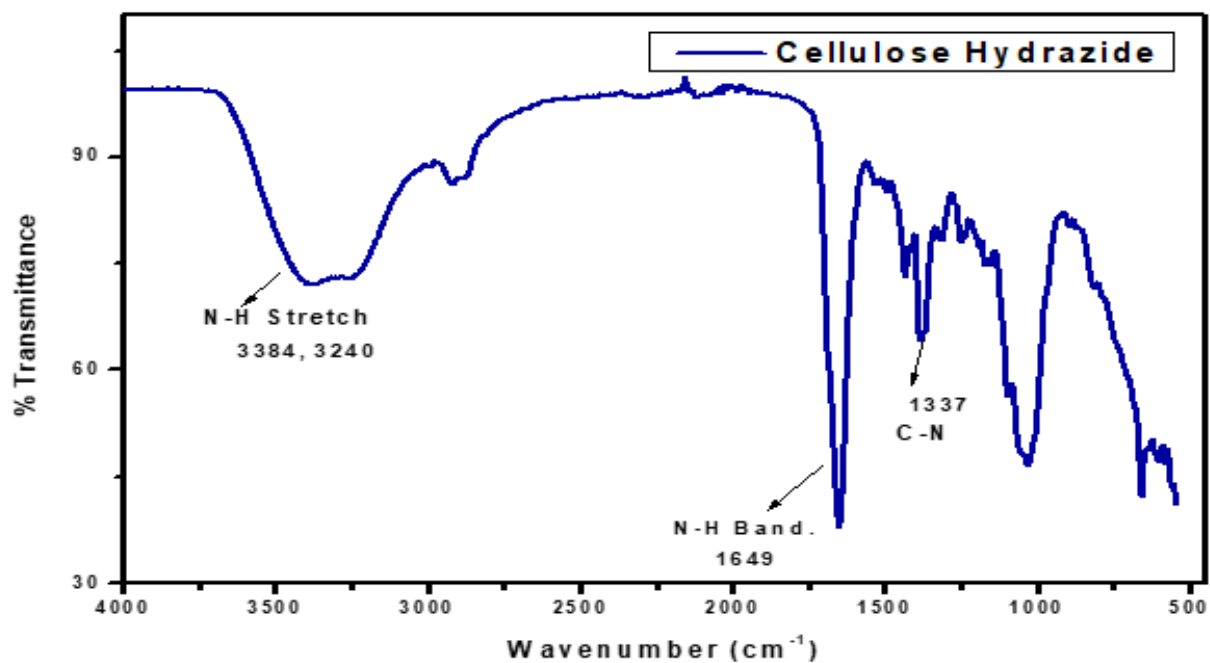
Figure 4.6 FT-IR of 6-deoxy cellulose hydrazide (MCC-Hyd).

FT-IR analysis of 6-deoxycellulose (N, N-diethyl) amine (cell-DEM) is shown in figure 4.7
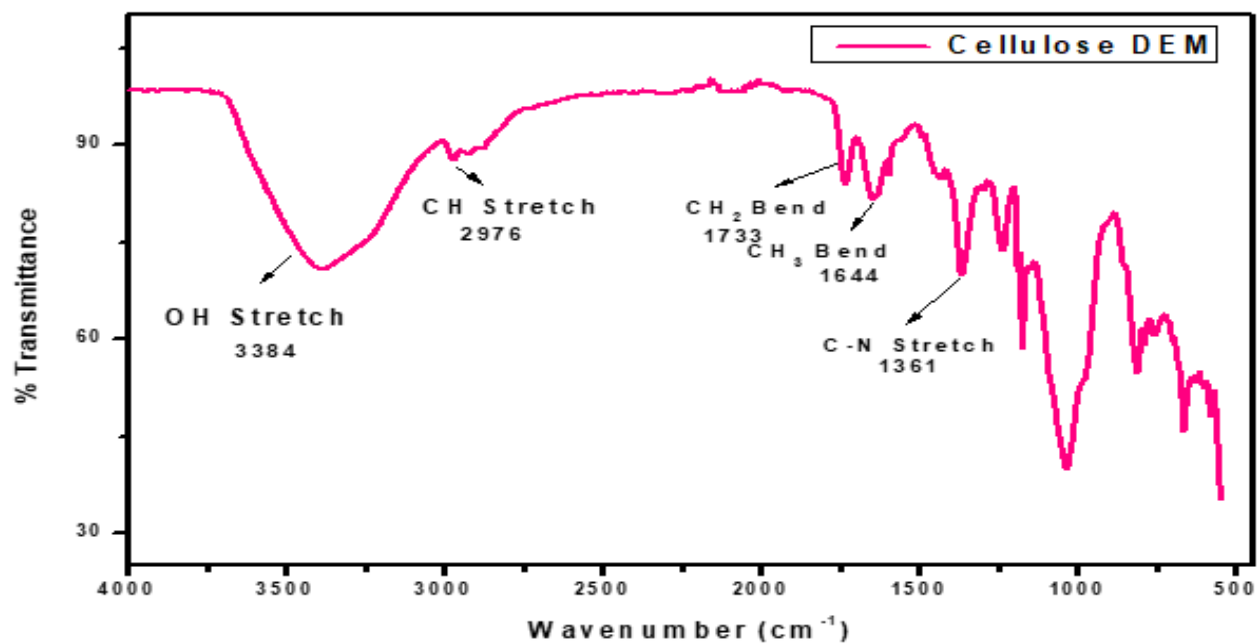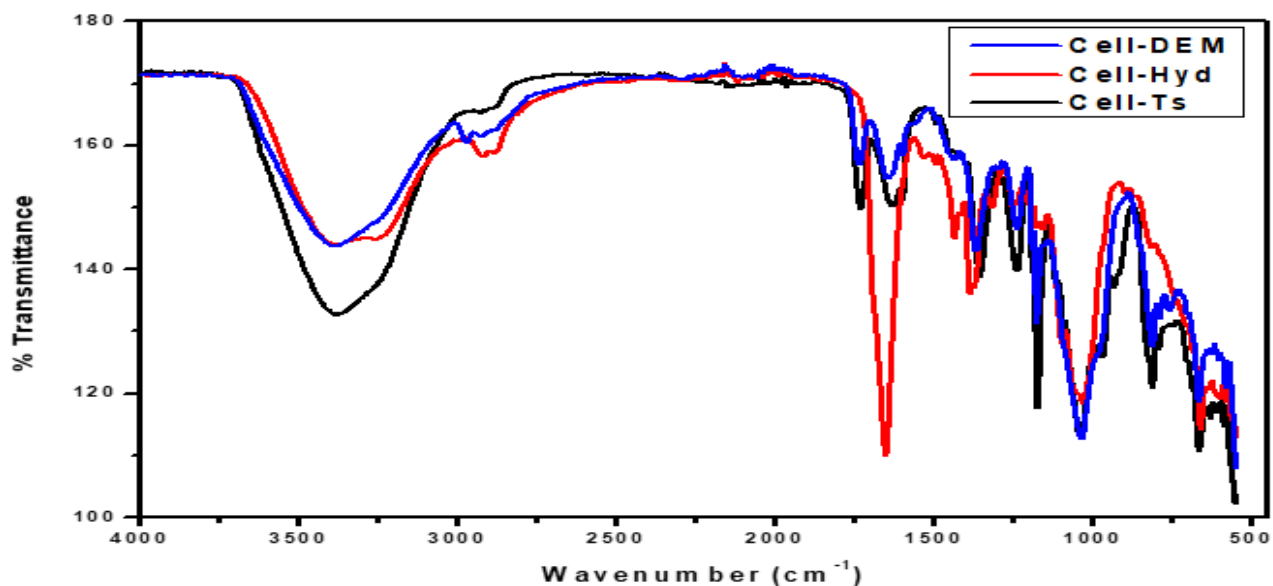

Figure 4.7 FT-IR of 6-deoxycellulose (N, N-diethyl) amine.

Following absorption bands has been observed for 6-deoxycellulose amine (N,N-diethylamine), a strong absorption band at 3384 cm^{-1} for –OH stretch, -CH stretch at 2976 cm^{-1}, 1733cm^{-1} and 1644cm^{-1} for –CH$_2$ and –CH$_3$ bend respectively. The strong band at 1361cm^{-1} confirms the presence of –C-N stretch.

Figure 4.8 Superimposed FT-IR Spectra.

4.2 Elemental Analysis:

Elemental analysis provides qualitative and quantitative analysis of samples. Determination of the major constituents of organic compounds specifically carbon, hydrogen and nitrogen is commonly done by CHN and CHNS analyzer. In this technique oxidative decomposition of organic compounds occur followed by reduction of sulfur oxides and nitrogen with the formation of end products. The resulting products are water, carbon dioxide, sulfur oxide and elemental nitrogen. In order to find the composition of particular element in compound, masses of these resulting products are used.[87]

Figure 4.9 Elemental Analyzer.

CHNS analysis of prepared samples were performed at model 240 CHN analyzer. Table 4.1 shows detail of CHNS of samples.

4.2.1 CHN Analysis:

Sr. No.	Sample Code	Weight	C%	H%	N%
1.	Cell-Hyd	0.0825	38.93	6.53	12.26
2.	Cell-DEM	0.0800	47.44	6.43	5.43
3.	TsMCC	0.0800	31.34	4.16	0

Table 4.1. CHN analysis of prepared products.

Table 4.2 shows S analysis of tosylated cellulose. Degree of tosylation was found to 42%.

4.2.2. S Analysis:

Sr. No.	Sample code	Weight	S%
1.	TsMCC	0.3013	4.49

Table 4.2. Sulphur analysis of Tosylated Cellulose.

4.3 XRD Analysis:

XRD is an analytical technique which is versatile and non-destructive and used form the analysis of crystalline materials. This technique allows the study of structure of the material which includes crystallite size, d-spacing and arrangement of atoms. In XRD analysis, monochromatic x-rays interact with crystalline sample. X-ray beam is generated in a cathode ray tube by heating the filament. These x-rays are then passed through monochromator to get monochromatic x-rays which are then focused on the material to be analyzed. X-rays reflect back after being targeted on the material and are detected by the detector which are then processed and converted into signals. XRD data can be used to determine the crystallite size by using the Scherer equation.[88]

Figure 4.10 XRD Instrument.

The XRD analysis of the samples were done in the range of 10^0 to 80^0 using a diffractometer with Cu-Kα (K = 1.5406 A^0) radiations at room temperature. The XRD spectra of MCC, OC, MCC-Hyd, and MCC-DEM are shown in **figure 4.11.** All the spectra show characteristic peaks of cellulose in corresponding spectra. The peak positions with corresponding lattice planes are given in table below.

| 2theta	Lattice planes
14.9	(11(-)0)
16.4	(110)
22.7	(200)
34.6	(004)

Table 4.3 XRD analysis of cellulose and derivatives.

Modified cellulose (OC, MCC-Hyd, and MCC-DEM) showed low crystallinity with characteristics near to the amorphous form as illustrated in figure 4.11 graph (b, c, d).
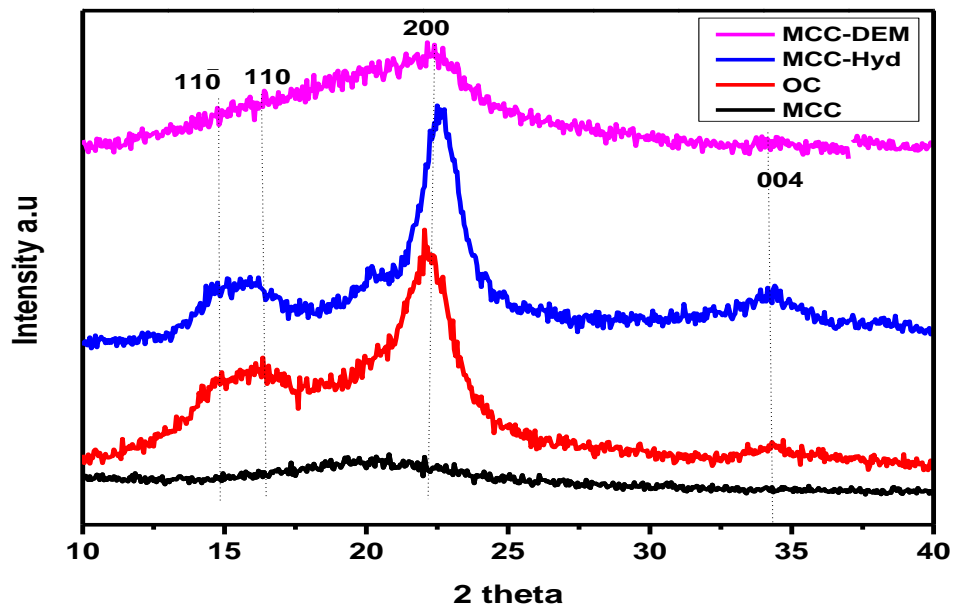
Figure 4.11. XRD Spectra of Bare (a) MCC, (b) OC, (c) MCC-Hyd, (d) MCC-DEM films.

Figure 4.12 graph (a, b, c, d) displays the XRD analysis of copper nanoparticles embedded films of MCC, OC, MCC-Hyd, and MCC-DEM respectively. All spectra shows additional peaks at 2θ $43.2°$ (111), $50.3°$ (200) and $73.9°$ (220) that are the distinctive diffraction peaks belongs to copper nanoparticles. Some additional peaks at 2θ $36.4°$, $42.2°$, $61.3°$ and $73.5°$ were also observed in these spectra. These may occurs due to the formation of copper oxide because copper readily oxidized to CuO and Cu_2O.
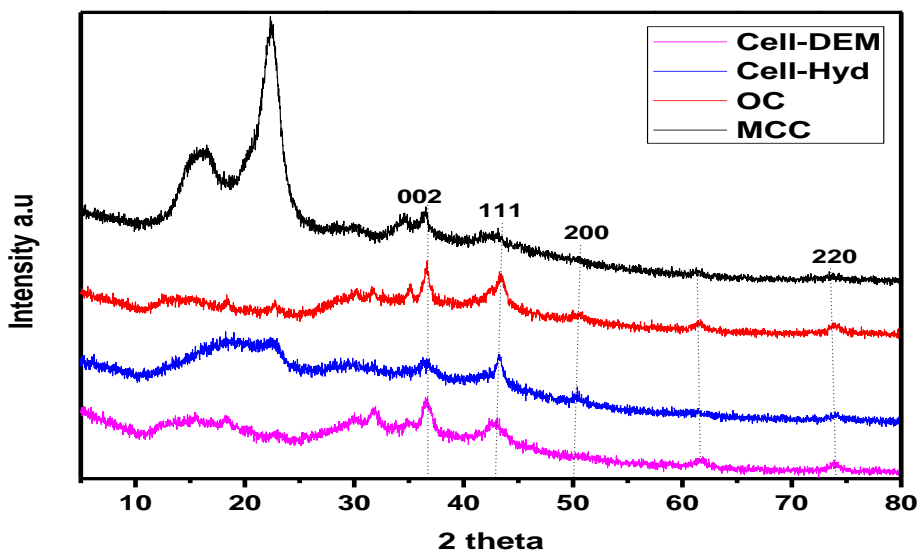


Figure 4.12. XRD Spectra of (a) Cu-MCC, (b) Cu-OC, (c) Cu-MCC-Hyd (d) Cu-MCC-DEM.

4.4 SEM Analysis:

Scanning Electron Microscopy is a non-destructive technique that gives valuable information about the structure, topography and composition of the given sample. It uses high energy beam of electrons that strike with the selective surface of the sample and produces back scattered electron, secondary electrons and diffracted back electrons that produces signal on the detector's screen.[89]

Figure 4.13 shows SEM images of all the prepared films embedded with nanoparticles. All images indicates the presence of small particles over the surface of films which confirms that nanoparticles are successfully template over the polymer support.
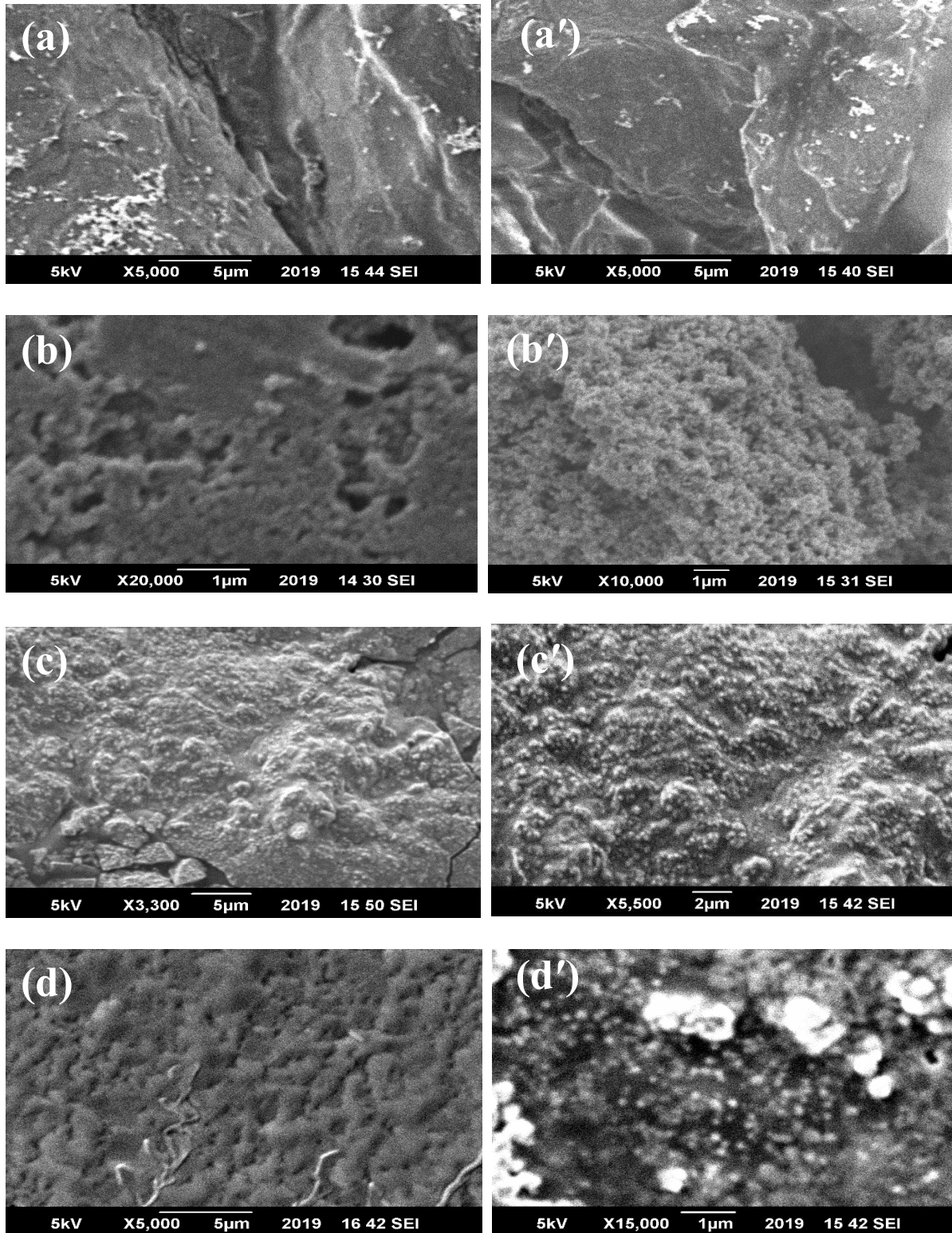
Figure 4.13 SEM images of all prepared films embaded with Cu nanoparticles. (a,a') MCC film (b,b') OC film (c,c') MCC-Hyd film (d,d') MCC-DEM film.

4.5 UV-VIS Spectroscopy:

UV spectroscopy is an important tool in quantitative determination of different analytes which absorb UV radiations. It is used in detection of presence or absence of chromosphere in analyte, conjugation of bonds and structure elucidation of compounds by measuring wavelength and absorbance.

When UV-Vis radiations fall on the molecule, absorption causes electronic excitations that occur from lower energy level to higher energy level. Electronic excitation occurs by absorption of specific wavelength for each kind of transitions in a molecule. Many factors play their role in absorption like conjugated system absorbs at higher wavelength and unconjugated system needs higher energy for absorption.[89]

Figure 4.14 UV-VIS spectrophotometer.

4.6 Degradation studies:

Degradation experiments were carried out on 4NP, Methyl orange, methylene blue and Congo red dye. For this purpose, a stock solution of 5Mm for 4NP and 0.1Mm for dyes (MO, MB, and CR) was made which was further diluted up to 0.05Mm and 0.08Mm for 4NP and dyes respectively, and degradation studies were carried out for all the prepared samples. For all catalysts $0.5cm^2 \times 1cm^2$ strips, 2.5ml of aqueous solution of dyes and 0.5ml of $NaBH_4$ solution was used. Reaction was carried out in quartz cuvette cell and spectra was recorded on spectrophotometer.

4.6.1 Degradation of 4-Nitrophenol:

First bare cellulose film was placed in UV cuvette containing 2.5ml of aqueous solution of 4NP and 0.5ml of NaBH4 and its spectra was recorded after every one minute till half an hour. Figure 4.15 (a) shows that no change in absorbance intensity at 400nm was observed. Which shows the poor catalytic performance of bare cellulose film towards the reduction of 4NP.

After that under similar conditions Cu^0 loaded strip was introduced to the cuvette containing reaction mixture. Change in color of 4NP was observed, it starts disappearing as soon as the Cu^0 strip was introduced. Fig. 4.15 (b) shows that absorbance intensity of peak at 400nm progressively decreases and completely disappeared after 19mints, show excellent catalytic reduction of 4NP by Cu^0 loaded cellulose film.
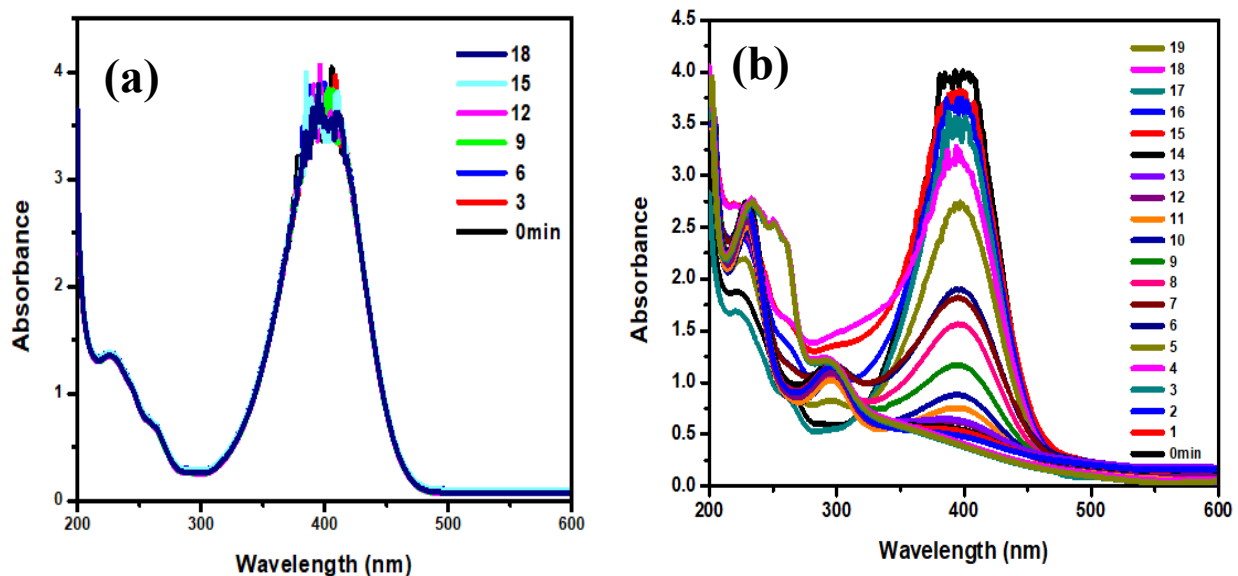
Figure 4.15 Absorption studies of 4-NP aqueous solution at various interval of time. (a) Bare MCC film (b) Cu-MCC film.
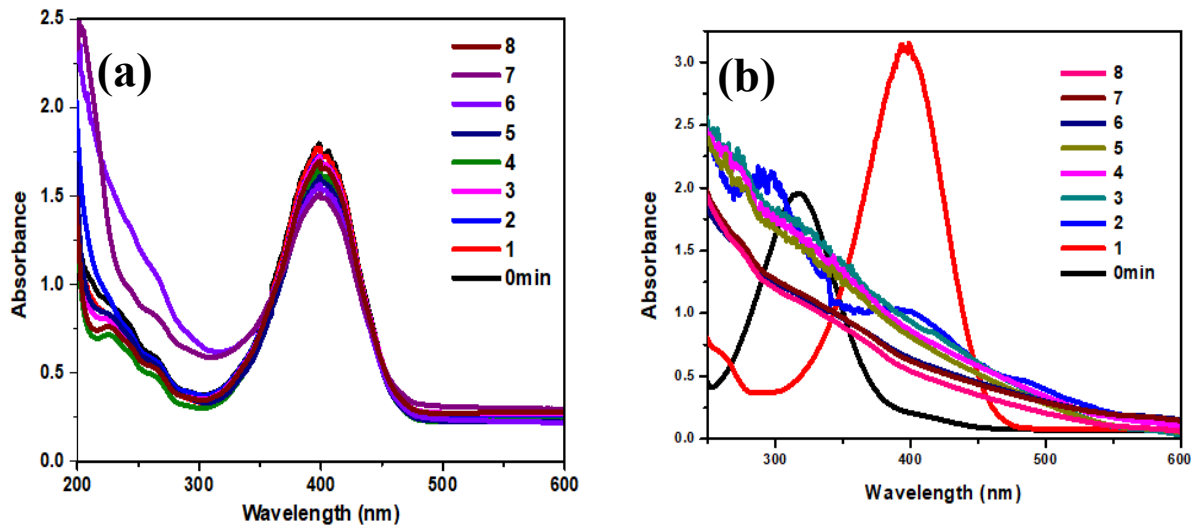
Figure 4.16 Absorption graph of 4-NP aqueous solution at various interval of time. (a) Bare OC film (b) Cu-OC film.

Degradation of 4-NP using oxidized cellulose film is shown n figure 4.16. Graph (a) shows no significant change in absorption intensity. While graph (b) shows a very rapid decrease in absorption intensity, presenting excellent catalytic performance. The absorption peaks completely disappear in 8 minutes.
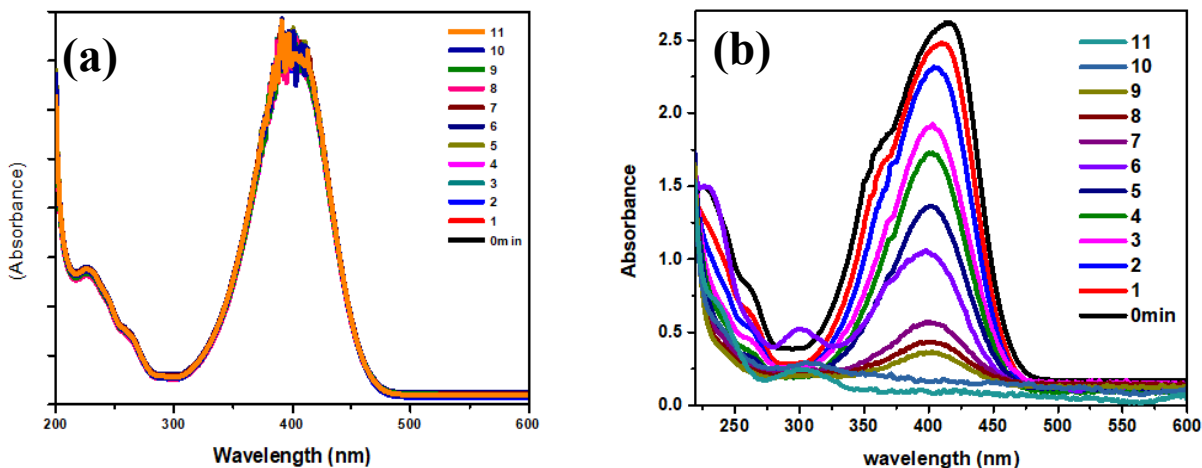

Figure 4.17 Absorption studies of 4-NP aqueous solution at various interval of time. (a) Bare MCC-HYd film. (b) Cu-MCC-Hyd film.
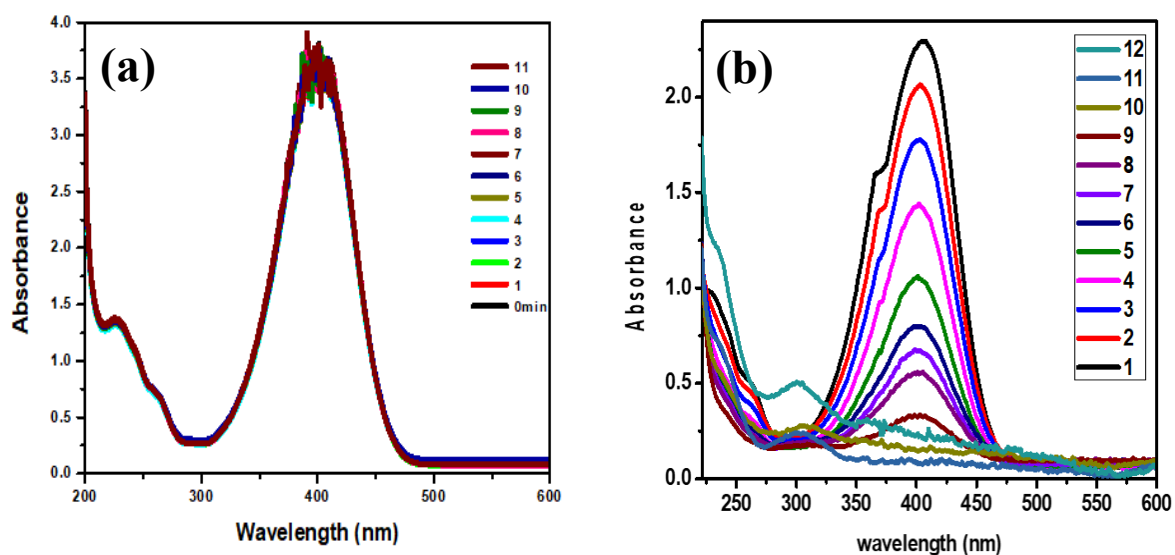
Figure 4.17 (a, b) shows degradation of 4-NP with bare MCC-Hyd and Cu^0 loaded MCC-Hyd film. No degradation has been observed with bare film. While gradual decrease in absorbance intensity at 400nm was observed with Cu^0-MCC-Hyd film. The absorption peak at 400nm vanishes completely after 11 minutes.

Figure 4.18 Absorption spectra of 4-NP at different interval of time. (a) Bare MCC-DEM film. (b) Cu-MCC-DEM film.

Degradation of 4-NP with MCC-DEM films is shown in figure 4.18. Graph (a) reveals no change in absorbance at wavelength 400nm showing no degradation. While Cu^0 –MCC-DEM shows change in absorbance peak at after every reading graph (b).the absorbance peak at 400nm wipe out after 12 minutes.

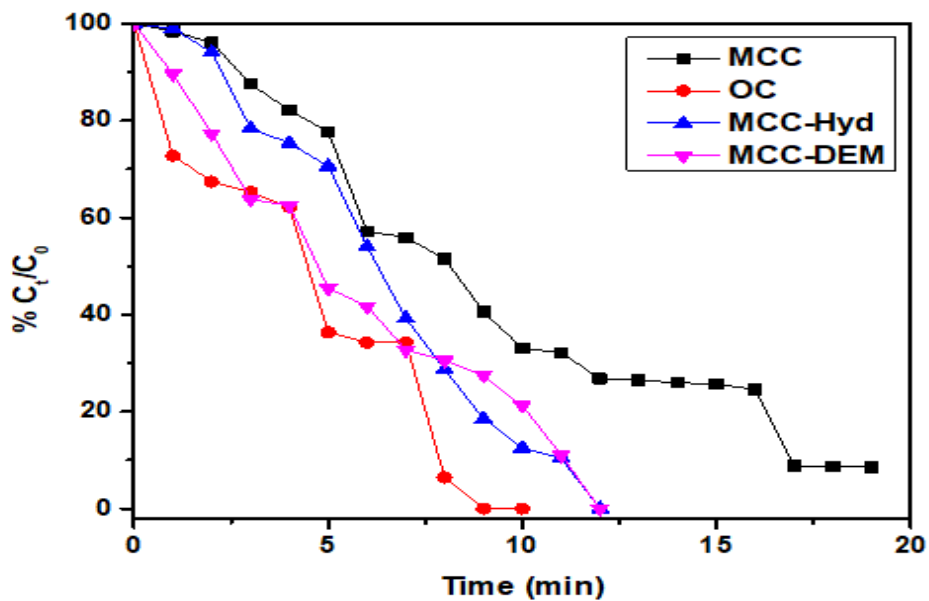*Figure 4.19 Activity of all prepared samples against 4-NP degradation.*

Figure 4.19 illustrate the activity of all the prepared samples against degradation of 4-Nitrophenol with the passage of time in terms of C_t/C_0. It can been seen that all samples show excellent efficiency but the highest efficiency is observed with Cu-OC in minimum time.
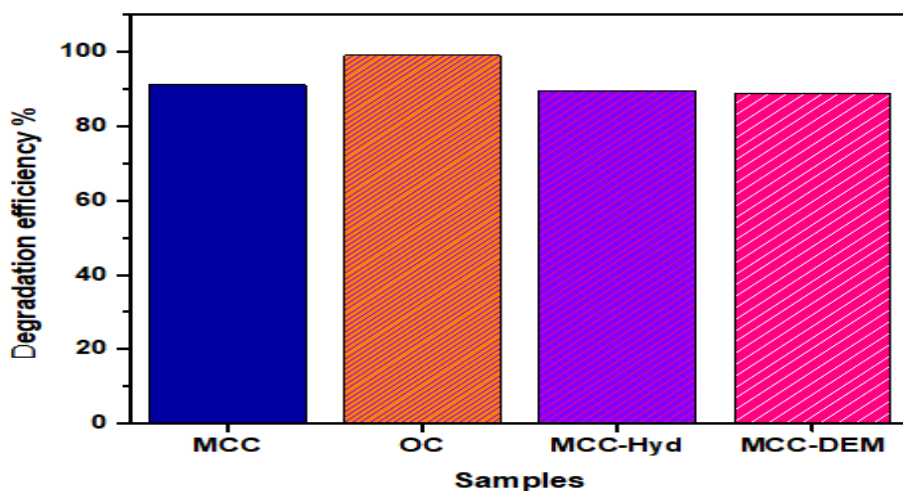

Figure 4.20 efficiency of all prepared samples against 4-NP degradation.

Figure 4.20 shows percentage degradation efficiency of all prepared films against 4-nitro phenol degradation. All ZVC Nps loaded films show excellent degradation efficiency, highest efficiency is achieved for OC i.e. 99%.

It was observed from the degradation studies of 4-Notrophenol that bare films showed very little or no degradation while all films loaded with ZVC nanoparticles revealed excellent degradation. And if films were compared with each other than OC loaded with ZVC nps show fastest catalytic degradation. While MCC-Hyd and MCC-DEM also takes less time as compared to pure MCC film. The reason for slow degradation by MCC film might be less adsorption of Cu^{+2} ions and in turns formation of less amount of ZVC nanoparticles. While modified cellulose (OC, MCC-Hyd, and MCC-DEM) provides more adsorption sites for metal ions and hence more ZVC nanoparticles are formed ultimately showing more and faster degradation.

4.6.2 Degradation of Congo red:

Similarly the degradation studies were carried out on Congo red using all the prepared films. The maximum and characteristics absorbance of Congo red is at 498nm. Figure 4.21 shows degradation studies of Congo red with bare MCC and Cu0 loaded MCC film. The decrease in absorbance after every reading is very evident from graph (b) plotted of quantity absorbed verses wavelength. 94% degradation has been observed in 11 minutes of catalytic activity.

Figure 4.21 Absorption Spectra of Congo red aqueous solution at different interval of time. (a) Bare MCC film. (b) Cu-MCC film.

Figure 4.22 Absorption Spectra of Congo red aqueous solution with (a) bare OC film. (b) Cu-OC film, at different interval of time.

Figure 4.22 shows degradation of Congo red with bare oxidized cellulose (OC) film. No change in absorbance means no degradation has been observed in the absence of Cu^0 nanoparticles graph (a). While a rapid decrease in absorbance intensity at 498nm has been observed showing rapid degradation. CR takes 10 minutes to degrade to 77.2% with Cu^0-OC film.

Figure 4.23 Absorption Spectra of Congo red aqueous solution with (a) bare MCC-Hyd film (b) Cu-MCC-Hyd film, at different interval of time.

Degradation spectra are shown in figure 4.23 for bare and Cu^0-MCC-Hyd. The drop in absorbance after every reading is evident from graph (b) plotted of quantity absorbed verses wavelength. 77.8 % degradation occurred in 8min presenting good catalytic performance.
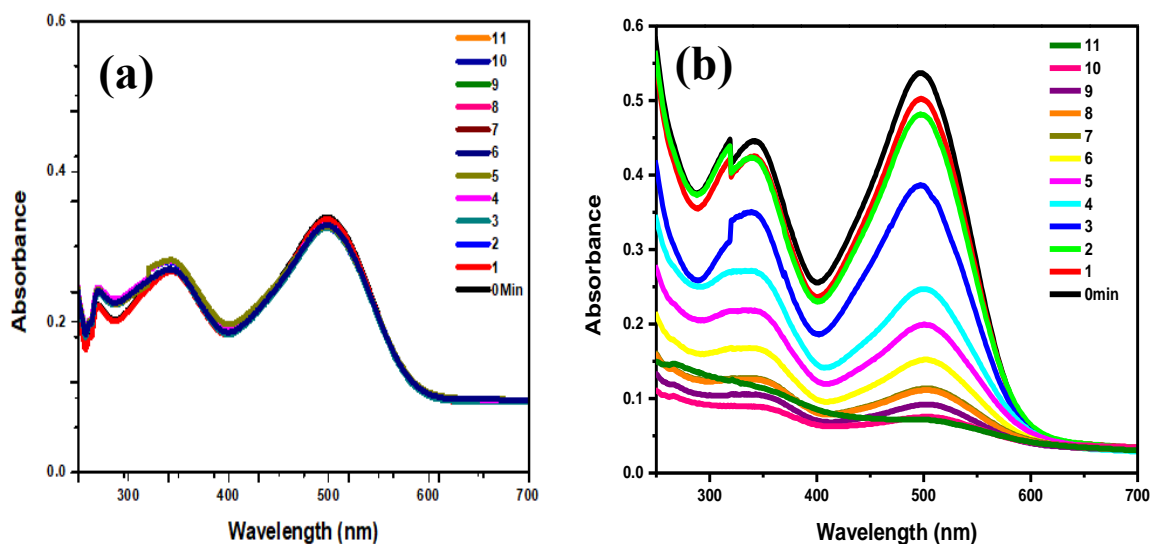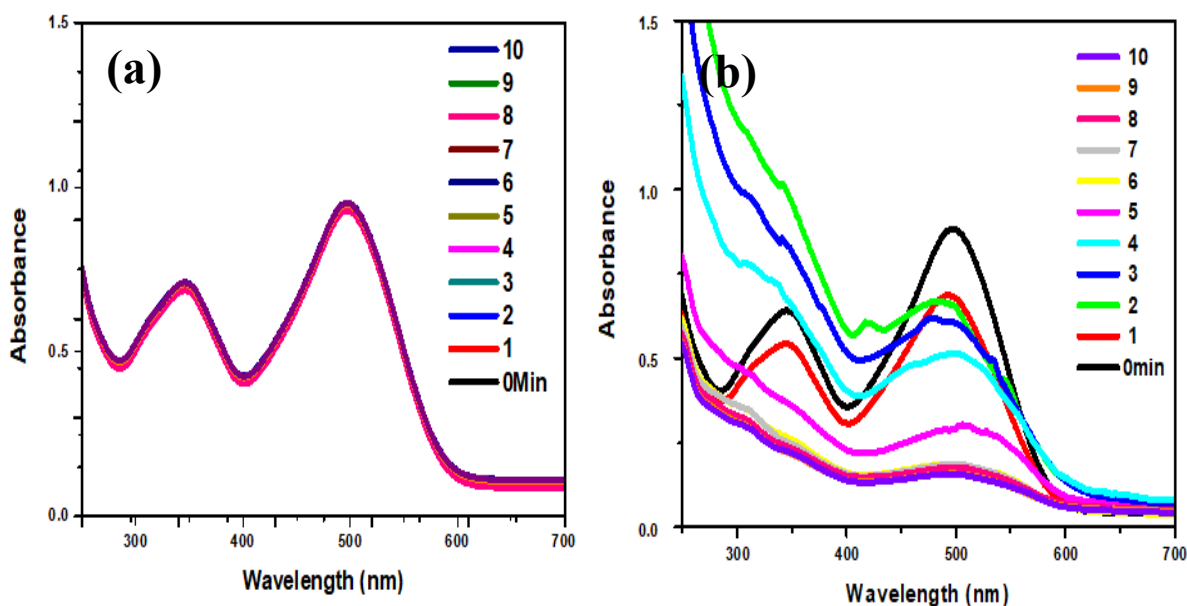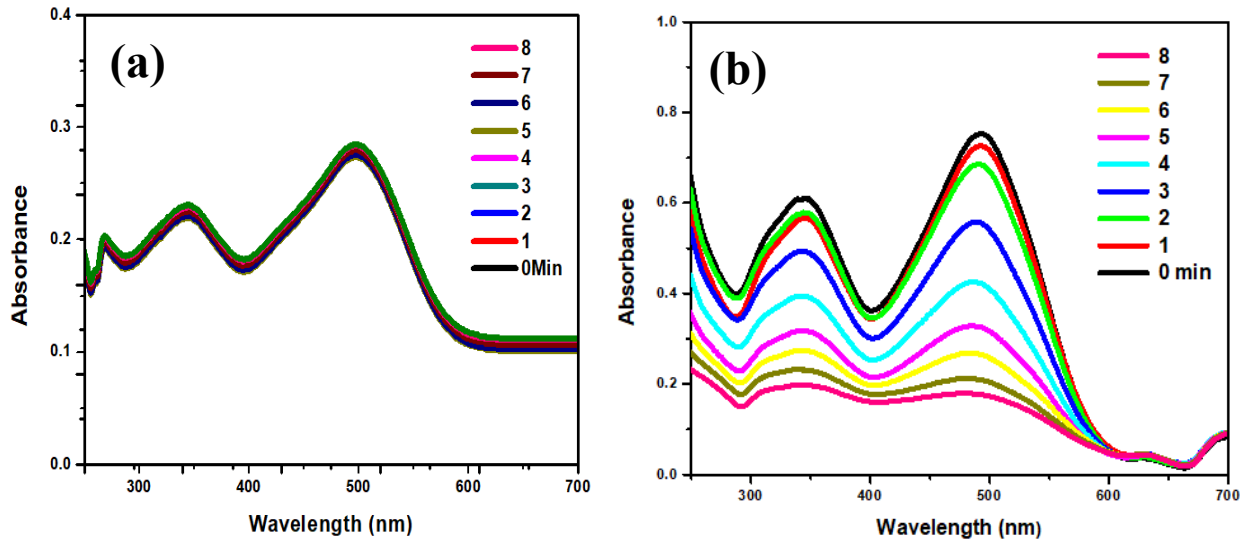

Figure 4.24 Absorption Spectra of Congo red aqueous solution at different interval of time.
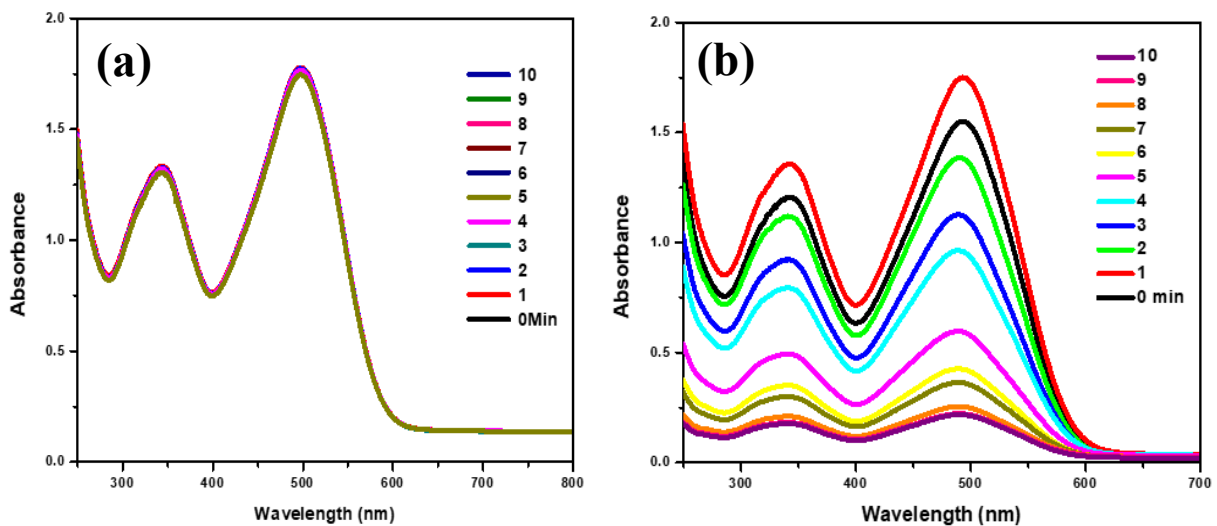*(a) Bare MCC-DEM film (b) Cu-MCC-DEM film.*

Figure 4.24 graph (b) depict gradual decrease in absorbance at wavelength 498nm after every minute. Cu^0-MCC-DEM takes 10 minutes to degrade CR to 91.2%.
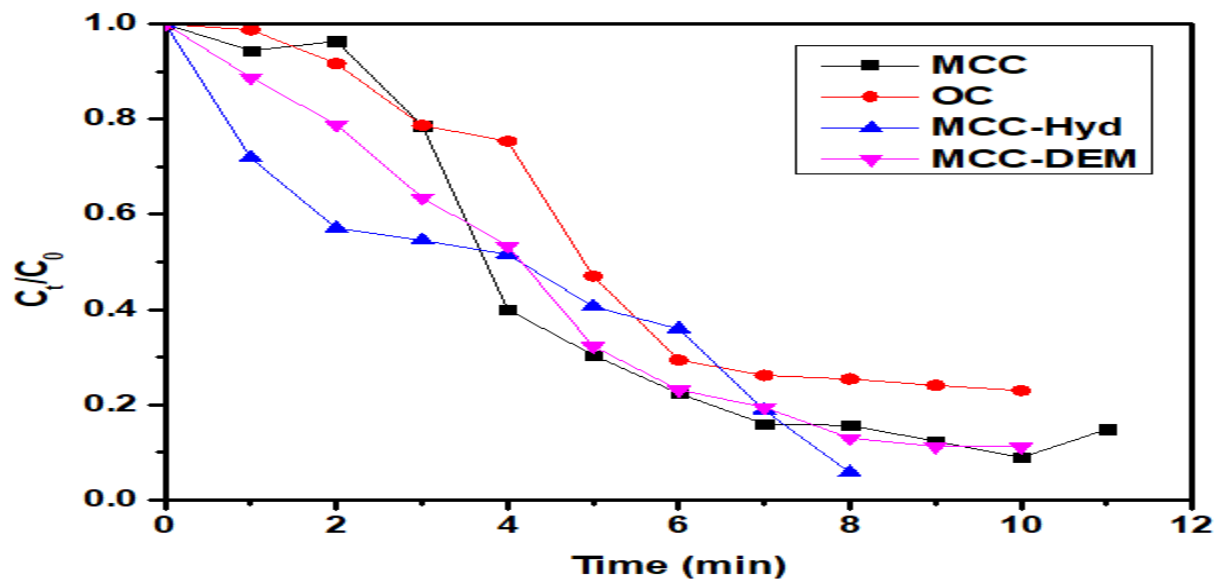
Figure 4.25. Activity of all films against CR degradation.

Figure 4.25 illustrate the activity of all the prepared samples against degradation of Congo red with the passage of time in terms of C_t/C_0. It can been seen that all samples show excellent efficiency but MCC-Hyd shows highest efficiency in minimum time.
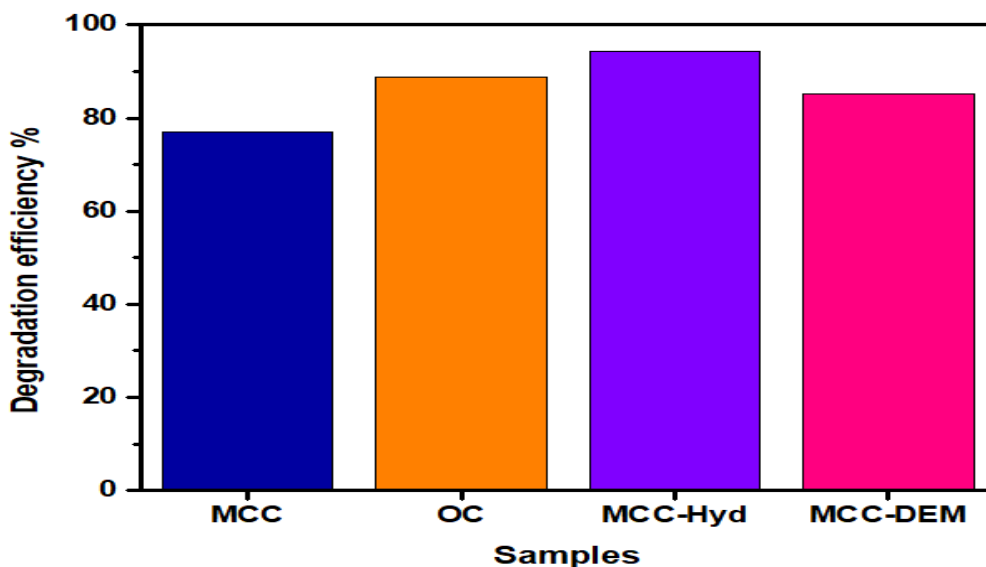
Figure 4.26 Efficiency of all prepared samples against CR degradation.

Percentage degradation efficiency of all prepared films against Congo red degradation is shown in figure 4.26. All ZVC Nps loaded films show excellent degradation efficiency, highest efficiency i.e. 94.2% is achieved MCC-Hyd.

4.6.3 Degradation of Methylene Blue:

Degradation studies were also carried out on methylene blue with all the prepared films under similar conditions. The maximum and characteristic absorbance intensity is at 664nm.

Degradation of MB with bare and Cu^0 loaded film is shown in figure 4.27. Graph (a) shows no change in absorbance intensity at 664nm till 21 minutes while graph (b) shows Reduction of MB in the existence of Cu^0 nanoparticles. Decrease in absorbance peak at 664nm shows degradation which has been completed in 19 minutes.

Figure 4.27 Absorption Spectra of Methylene blue aqueous solution at different interval of time (a) bare MCC film (b) Cu-MCC film.

Figure 4.28 Absorption spectra of Methylene blue aqueous solution at different interval of time. (a) Bare OC film (b) Cu-OC film.

Figure 4.28 graph (b) shows rapid decline in absorbance peak at wavelength 664nm. The reduction of absorbance intensity with the passage of time revealed fast degradation which completes in 9 minutes.

Figure 4.29 Absorption Spectra of Methylene blue aqueous solution at different interval of time. (a) Bare MCC-Hyd film (b) Cu-MCC-Hyd film.

Figure 4.30 Absorbance Spectra of Methylene blue aqueous solution at different interval of time. (a) Bare MCC-DEM (b) Cu-MCC-DEM.

Similarly, figure 4.29 and 4.30 shows degradation spectra of methylene blue with amino modified cellulose MCC-Hyd and MCC-DEM respectively. Cu^0-MCC-Hyd takes 11 min while Cu^0-MCC-DEM takes 13 min to degrade MB to 94% and 91% respectively.
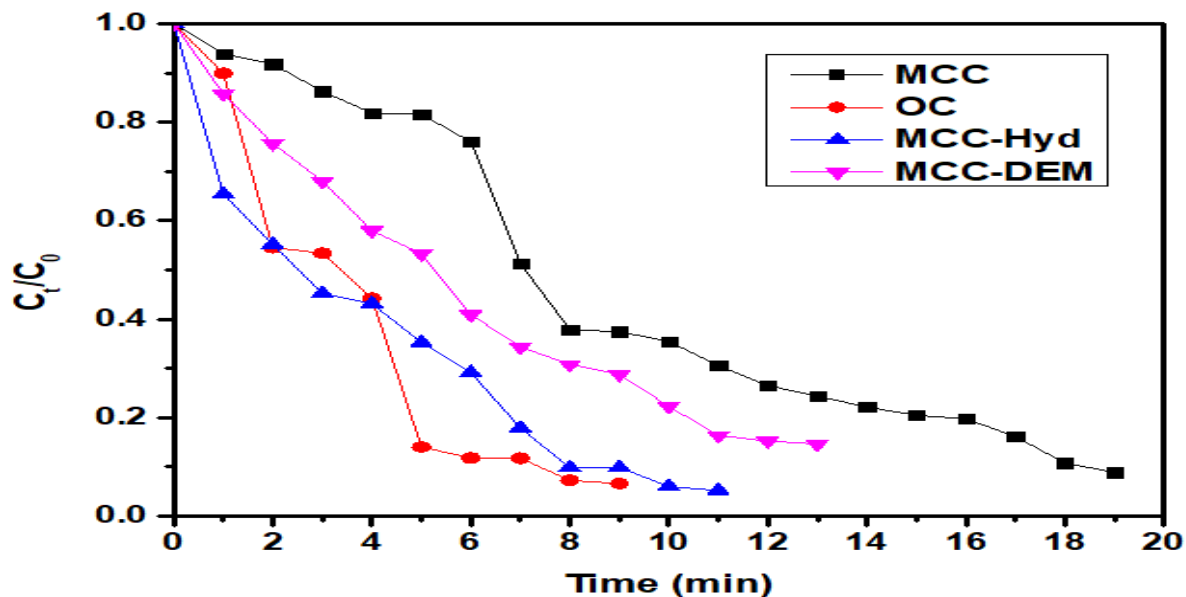
Figure 4.31 Activity of all prepared samples against MB degradation.

Figure 4.31 illustrate the activity of all the prepared samples against degradation of MB with the passage of time in terms of C_t/C_0. It can be observed that all samples show efficient degradation but OC and MCC-Hyd shows highest efficiency in minimum time.
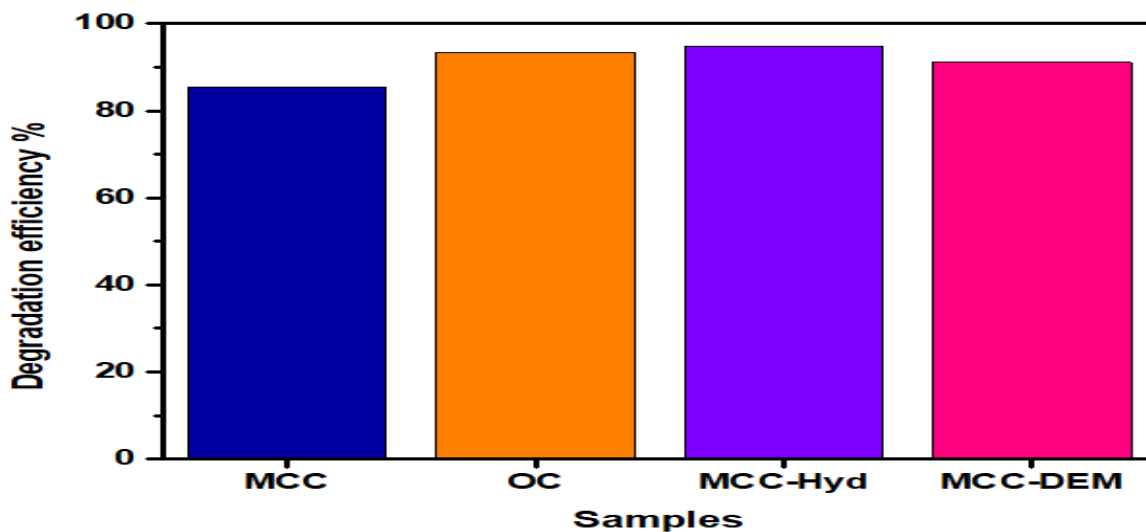
Figure 4.32 Efficiency of all films against MB degradation.

Figure 4.32 shows the degradation efficiency of all the prepared films against MB degradation in terms of perentage. Graph revealed OC and MCC-Hyd derivatives of Cellulose in the presence of ZVC nanoparticles.

4.6.4 Degradation of Methyl orange:

Methyl orange was also degraded using all the prepared films with and without zero-valent copper nanoparticles. 2.5ml of aqueous solution of MO and $0.5cm^2 \times 1cm^2$ film was placed in UV cuvette, 0.5ml of $NaBH_4$ solution was added and its absorption spectra was recorded on UV-VIS spectrophotometer.

Figure 4.33 graph (a) shows no change in absorption spectrum revealing that $NaBH_4$ alone cannot degrade MO. While in graph (b) gradual decrease in absorbance intensity is observed after every reading. The absorbance peak diminishes completely after 12 minutes.
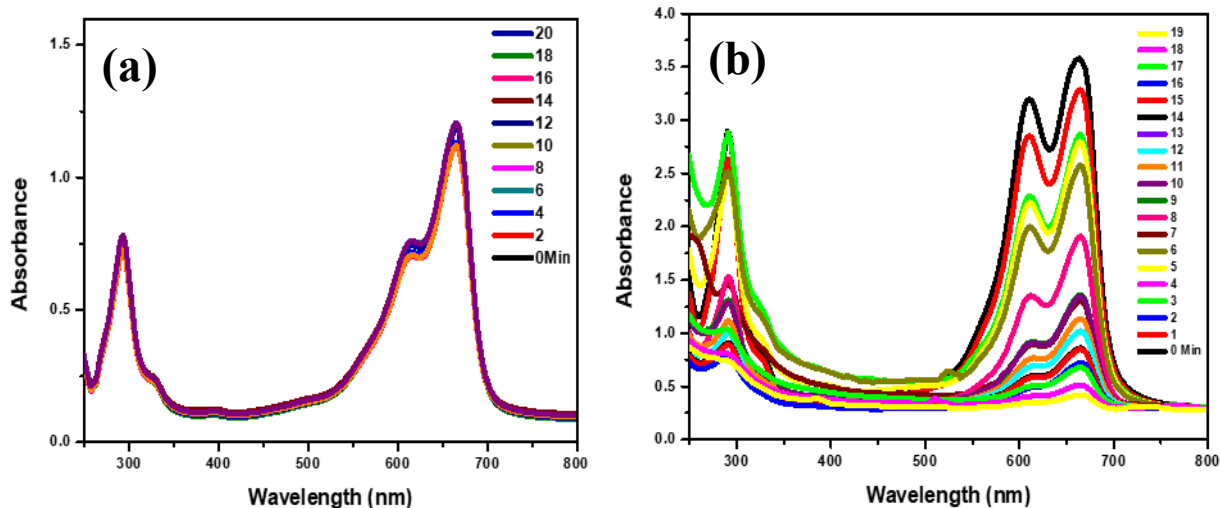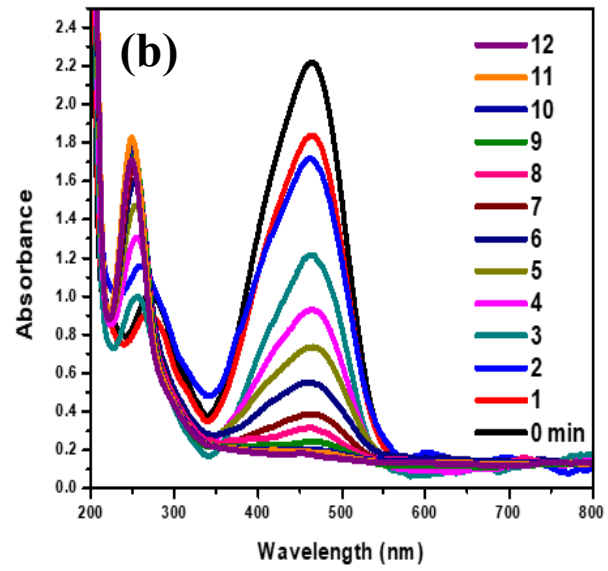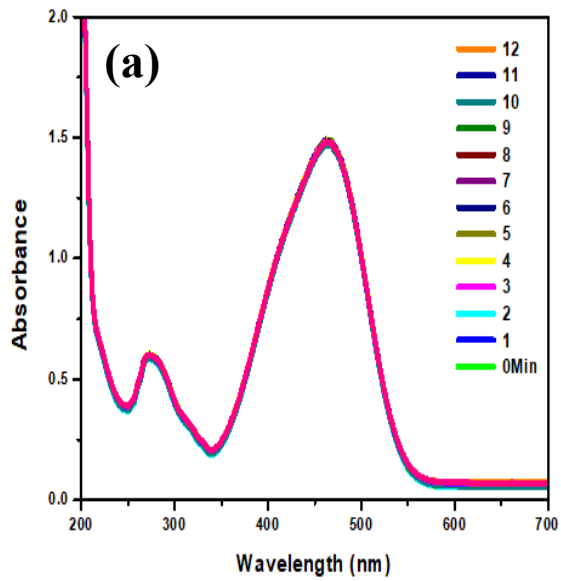
Figure 4.33 Absorption Spectra of Methyl Orange aqueous solution at different interval of time. (a) Bare MCC film (b) Cu-MCC film.
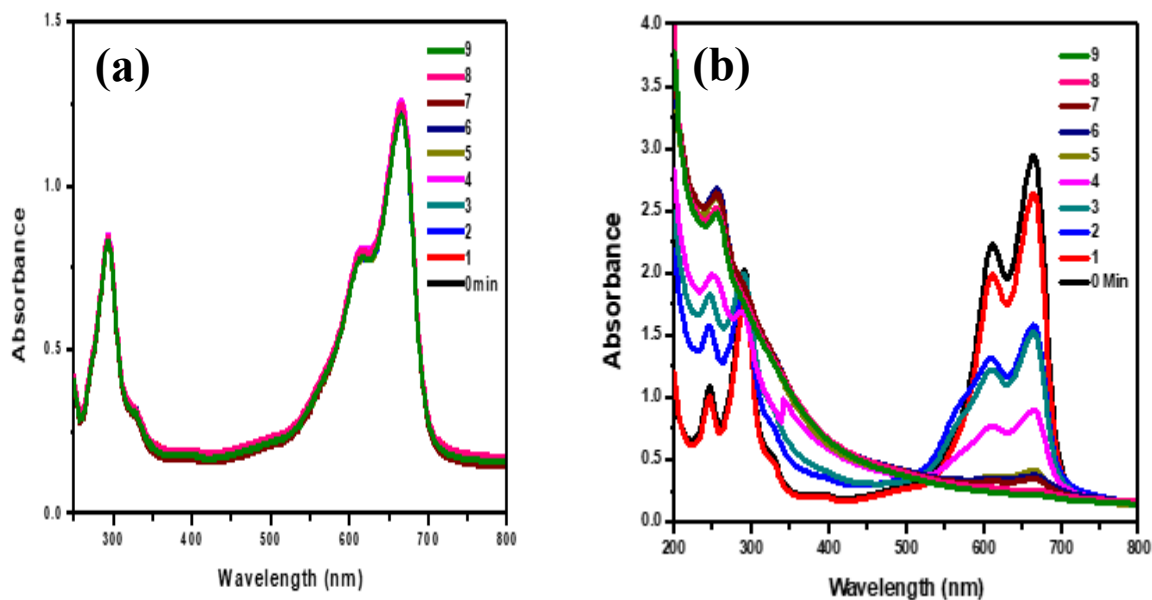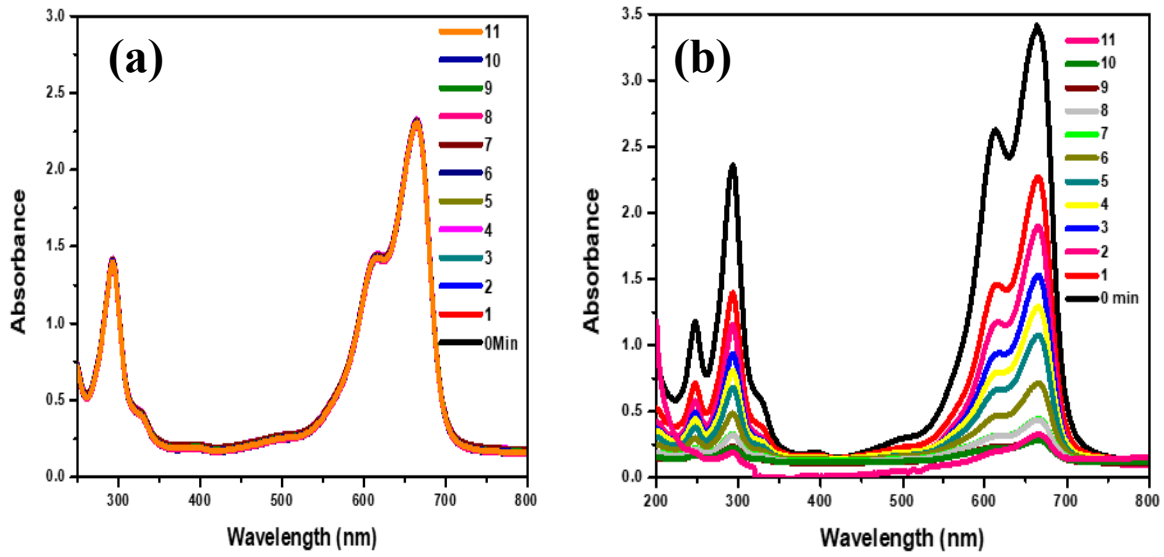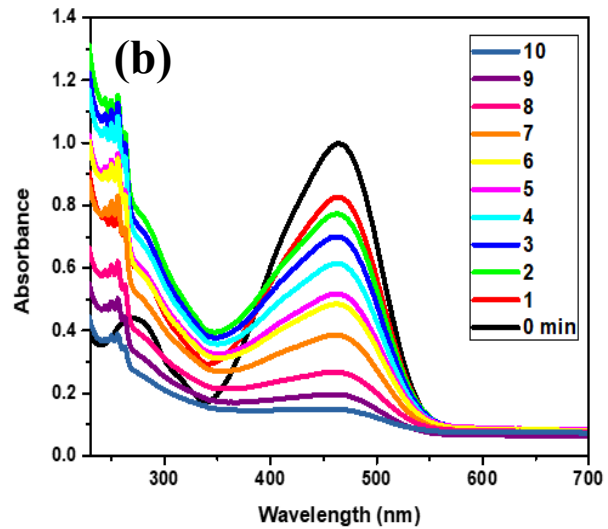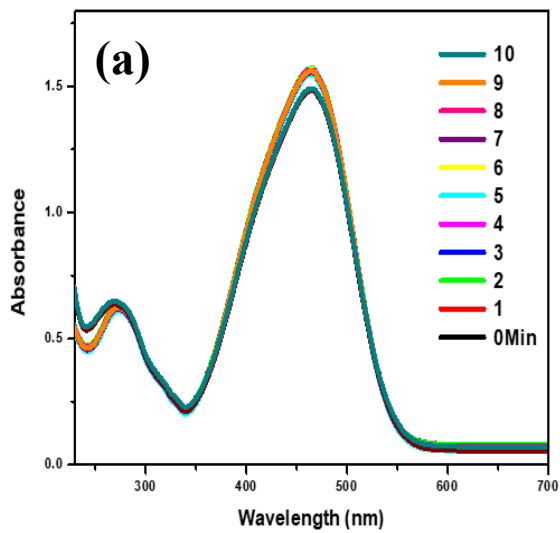

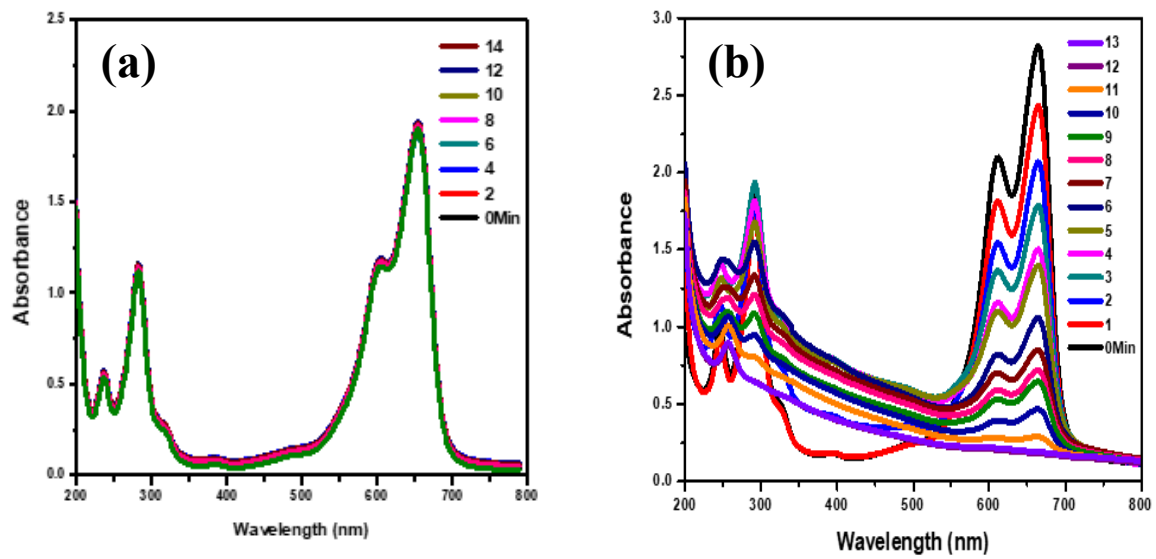*Figure 4.34 absorption spectra of Methyl orange aqueous solution at different interval of time. (a) Bare OC film (b) Cu-OC film.*
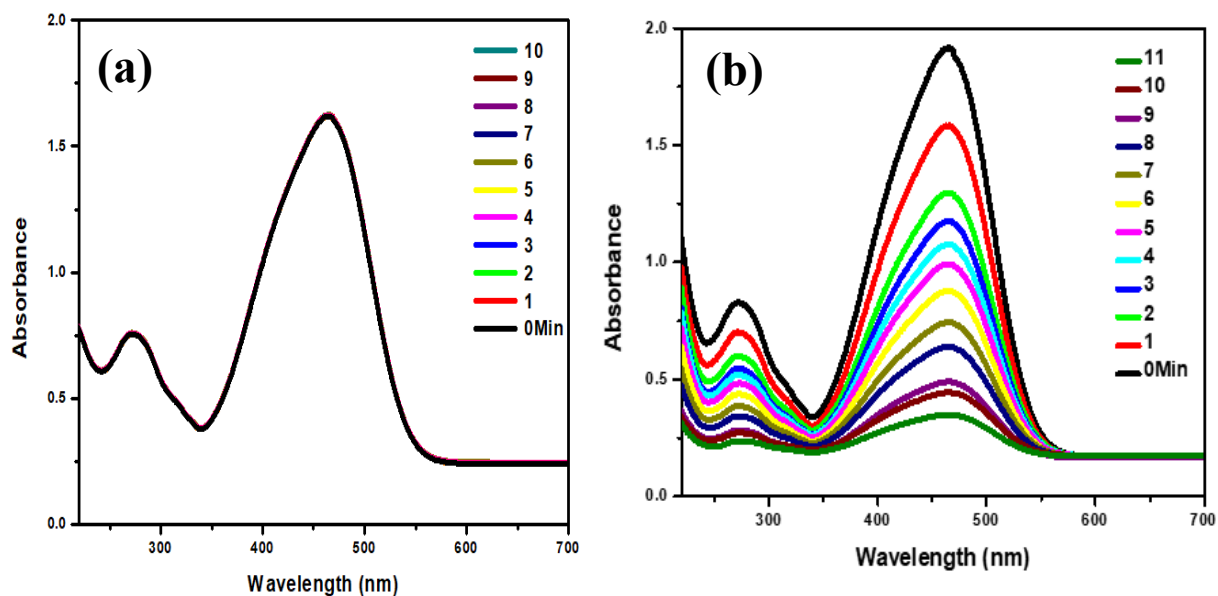
Figure 4.35 Absorption Spectra of Methyl orange aqueous solution at different time interval. (a) Bare MCC-Hyd film (b) Cu-MCC-Hyd film.
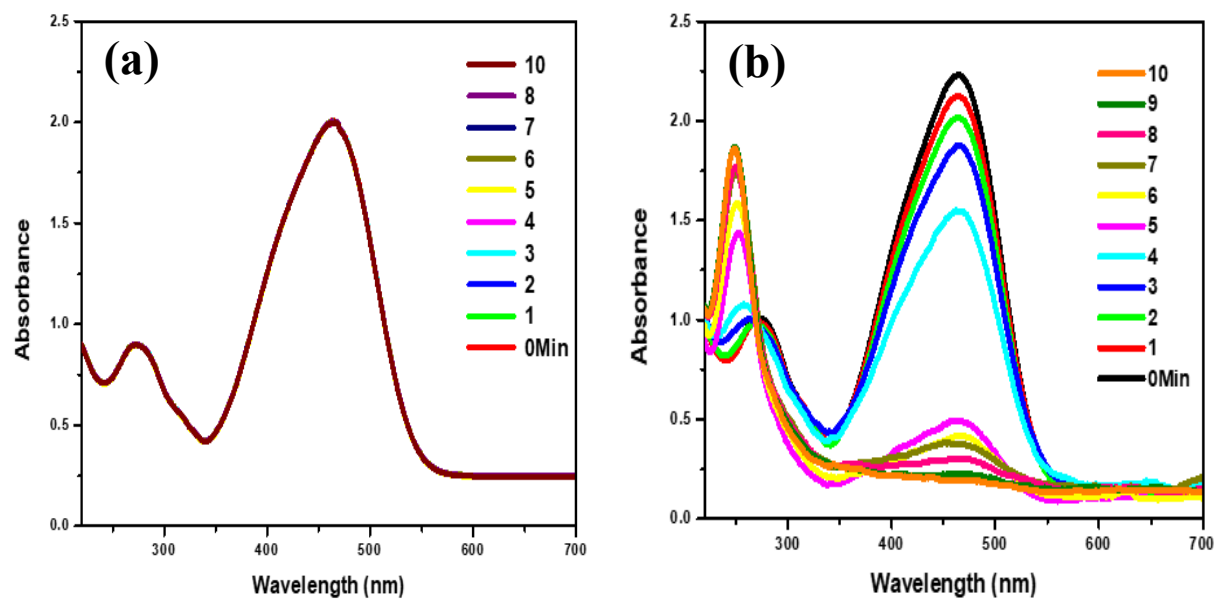

Figure 4.36 Absorption spectra of Methyl orange aqueous solution at different time interval. (a) Bare MCC-DEM film (b) Cu MCC-DEM film.

Similarly, figure 4.34, 4.35 and 4.36 shows degradation spectra of methyl orange with oxidized cellulose (OC), MCC-Hyd and MCC-DEM respectively. No change in absorbance occurred in the absence of zero valent nanoparticles while decrease in absorbance with the passage of time was observed with Cu^0 loaded films.
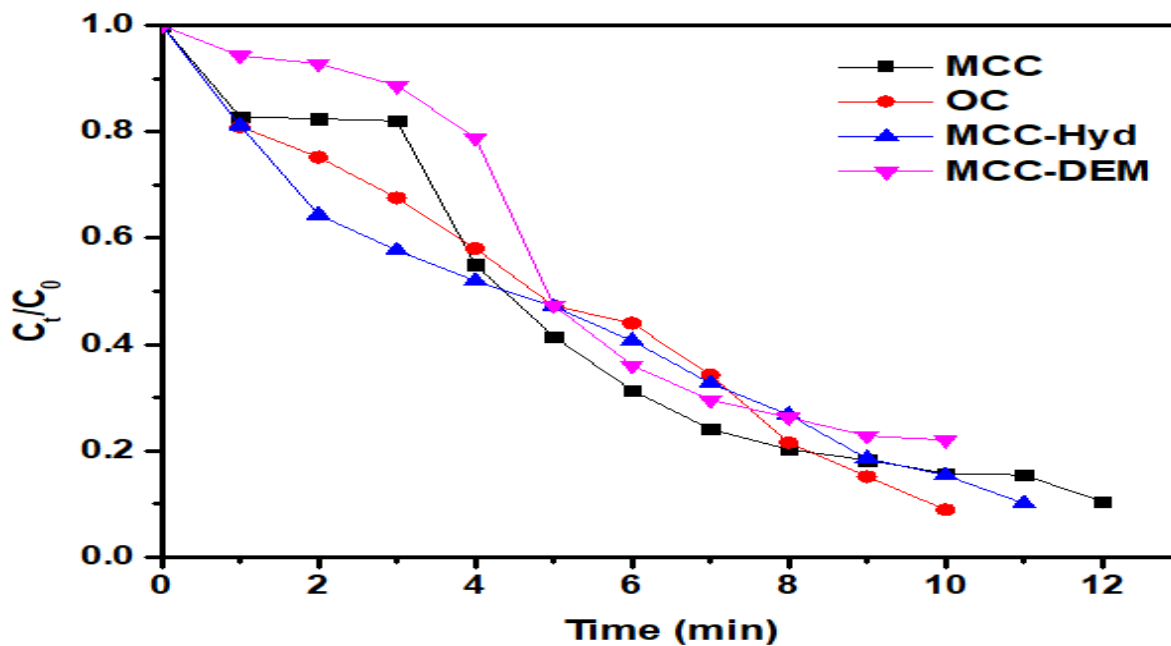
Figure 4.37 Activity of all prepared films against MO degradation.

Figure 4.37 illustrate the activity of all the prepared samples against methyl orange degradation at different interval of time in terms of C_t/ C_0. It can been seen that all samples show excellent. Cu^0-OC and Cu^0-MCC-Hyd takes minimum time to degrade.
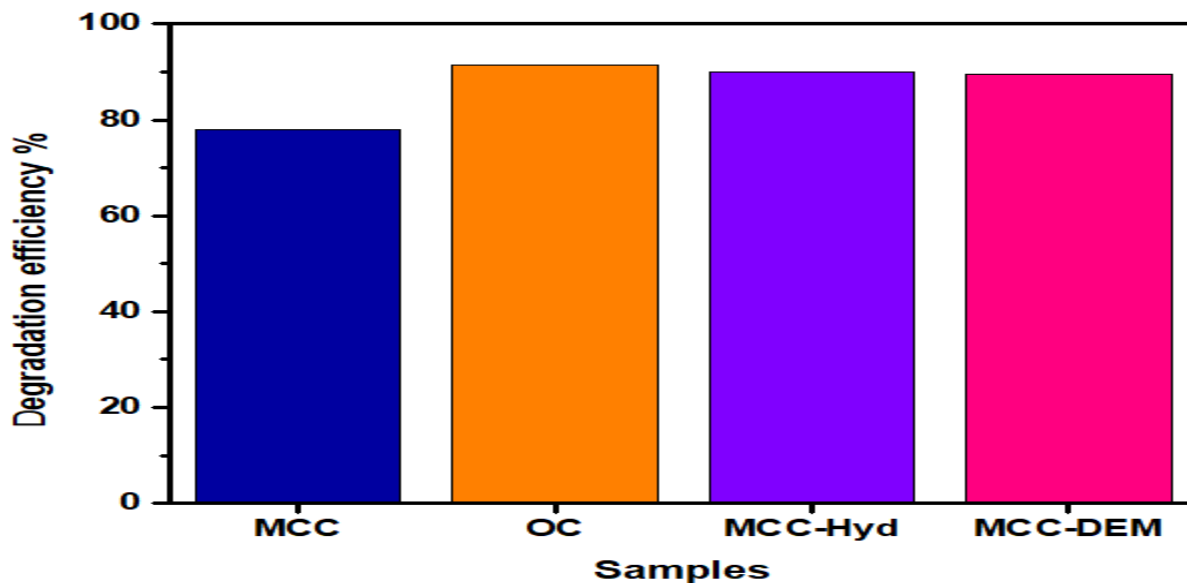
Figure 4.38 Efficiency of all prepared films against MO Degradation.

Percentage efficiency of all the films against methyl Orange degradation is shown in figure 4.38. All ZVC embedded films showed efficient degradation. While the efficiency of ZVC OC, MCC-Hyd and MCC-DEM is comparable. Highest efficiency is for 91.3% for OC.
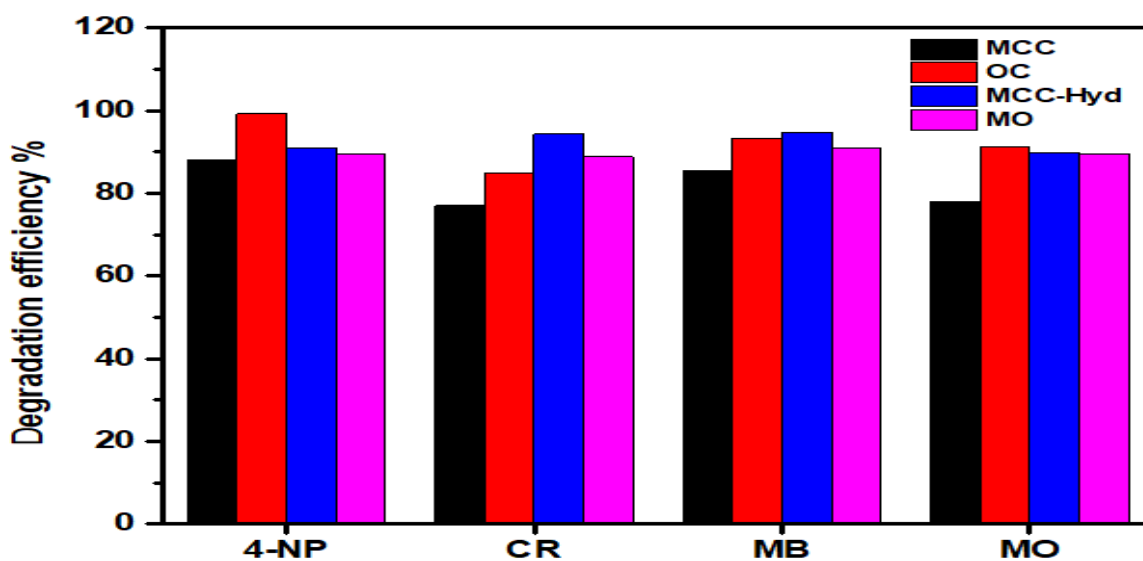
Figure 4.39 Comparison percentage efficiencies of all the samples against all dyes.

Figure 4.39 illustrates the percentage efficiencies of all the samples for all four dyes. Graphs shows that Modified cellulose showed excellent degradation efficiency for all dyes. Oxidized cellulose showed highest efficiency in almost all cases. While amino modified derivatives also exhibit more than 85% efficiency in all cases.

4.7 Summary of results:

Sr. No.	Samples/films	4-NP		CR		MB		MO	
		% deg.	time	% deg.	time	% deg.	time	% deg.	time
1.	MCC	88	19	77	11	85.4	10	77.9	12
2.	OC	99	8	85	10	93.4	9	91.3	10
3.	MCC-Hyd	91	11	94.2	8	94.8	11	89.9	11
4.	MCC-DEM	89.6	12	88.8	10	91	13	89.5	10

Table 4.4. Summary of all results.

Conclusion:

➤ Here acid and amino modified cellulose named oxidized cellulose (OC), 6-Deoxycellulose hydrazide (MCC-Hyd) and 6-deoxycellulose (N, N-diethyl) amine has been successfully synthesized.

➤ Cellulose and its synthesized derivatives were employed for uptake of copper ions from aqueous solution.

➤ Films of cellulose and modified cellulose was successfully prepared and used as supporting site for the production of zero valent copper nanoparticles.

➤ Chemical reduction method was used for the synthesis of Zero valent copper nanoparticles.

➤ OC, MCC-Hyd and MCC-DEM showed excellent degradation efficiency in the presence of Cu^0 nanoparticles.

References

1.   Younger, M., et al., *The built environment, climate change, and health: opportunities for co-benefits.* American journal of preventive medicine, 2008. **35**(5): p. 517-526.

2.   Lo, K., *A critical review of China's rapidly developing renewable energy and energy efficiency policies.* Renewable and Sustainable Energy Reviews, 2014. **29**: p. 508-516.

3.   Rashed, M.N., *Organic Pollutants: Monitoring, Risk and Treatment.* 2013: BoD–Books on Demand.

4.   Cheng, J., S. Dai, and X. Ye, *Spatiotemporal heterogeneity of industrial pollution in China.* China Economic Review, 2016. **40**: p. 179-191.

5.   Varavipour, M., T. Asadi, and M. Mashal, *Application of two layers of soil with different textures for decreasing pollution from landfills to the subterranean water table.* RESEARCH ON CROPS, 2011. **12**(3): p. 833-838.

6.   Jeyaratnam, J., *Health problems of pesticide usage in the Third World.* British journal of industrial medicine, 1985. **42**(8): p. 505.

7.   Kazi, T., et al., *Assessment of water quality of polluted lake using multivariate statistical techniques: A case study.* Ecotoxicology and environmental safety, 2009. **72**(2): p. 301-309.

8.   Regadío, M., et al., *Containment and attenuating layers: an affordable strategy that preserves soil and water from landfill pollution.* Waste management, 2015. **46**: p. 408-419.

9.   Agrawal, A., R.S. Pandey, and B. Sharma, *Water pollution with special reference to pesticide contamination in India.* Journal of Water Resource and Protection, 2010. **2**(05): p. 432.

10.   Haines, A., et al., *Climate change and human health: impacts, vulnerability and public health.* Public health, 2006. **120**(7): p. 585-596.

11.   Mekhilef, S., R. Saidur, and A. Safari, *A review on solar energy use in industries.* Renewable and Sustainable Energy Reviews, 2011. **15**(4): p. 1777-1790.

12.   He, G., M. Fan, and M. Zhou, *The effect of air pollution on mortality in China: Evidence from the 2008 Beijing Olympic Games.* Journal of Environmental Economics and Management, 2016. **79**: p. 18-39.

13.   Raaschou-Nielsen, O., et al., *Air pollution and lung cancer incidence in 17 European cohorts: prospective analyses from the European Study of Cohorts for Air Pollution Effects (ESCAPE).* The lancet oncology, 2013. **14**(9): p. 813-822.

14.   Järup, L., *Hazards of heavy metal contamination.* British medical bulletin, 2003. **68**(1): p. 167-182.

15.   Zawierucha, I., C. Kozlowski, and G. Malina, *Immobilized materials for removal of toxic metal ions from surface/groundwaters and aqueous waste streams.* Environmental Science: Processes & Impacts, 2016. **18**(4): p. 429-444.

16.   Rai, P.K., *Heavy metal pollution in aquatic ecosystems and its phytoremediation using wetland plants: an ecosustainable approach.* International journal of phytoremediation, 2008. **10**(2): p. 133-160.

17.   Longevialle, P. and O. Lefèvre, *Ion–neutral reorientation and unimolecular loss of alkanes from organic ions in the gas phase.* Organic mass spectrometry, 1993. **28**(10): p. 1083-1086.

18.   Yun, C.H., et al., *Hollow fiber solvent extraction removal of toxic heavy metals from aqueous waste streams.* Industrial & engineering chemistry research, 1993. **32**(6): p. 1186-1195.

19.   Babel, S. and T.A. Kurniawan, *Low-cost adsorbents for heavy metals uptake from contaminated water: a review.* Journal of hazardous materials, 2003. **97**(1-3): p. 219-243.

20.   Mohod, C.V. and J. Dhote, *Review of heavy metals in drinking water and their effect on human health.* International Journal of Innovative Research in Science, Engineering and Technology, 2013. **2**(7): p. 2992-2996.

21.   Sigel, A. and H. Sigel, *Metal Ions in Biological Systems: Volume 34: Mercury and its Effects on Environment and Biology*. 1997: CRC Press.

22.   Network, C.s.E.H., et al., *Training Manual on Pediatric Environmental Health: Putting it Into Practice*. 1999: Children's Environmental Health Network.

23.   Barakat, M., *New trends in removing heavy metals from industrial wastewater.* Arabian journal of chemistry, 2011. **4**(4): p. 361-377.

24.   Andleeb, S., et al., *Biological treatment of textile effluent in stirred tank bioreactor.* Int. J. Agric. Biol, 2010. **12**(2): p. 256-260.

25. Akpor, O.B., G.O. Ohiobor, and T.D. Olaolu, *Heavy metal pollutants in wastewater effluents: sources, effects and remediation.* Advances in Bioscience and Bioengineering, 2014. **2**(4): p. 37-43.

26. Cheriti, A., et al., *Copper ions biosorption properties of biomass derived from Algerian Sahara plants.* Expanding issues in desalination. Intech, 2011: p. 319-338.

27. Vunain, E., A. Mishra, and B. Mamba, *Dendrimers, mesoporous silicas and chitosan-based nanosorbents for the removal of heavy-metal ions: a review.* International journal of biological macromolecules, 2016. **86**: p. 570-586.

28. Xu, X.-R., et al., *Degradation of dyes in aqueous solutions by the Fenton process.* Chemosphere, 2004. **57**(7): p. 595-600.

29. Pauling, L., *A Theory of the Color of Dyes.* Proceedings of the National Academy of Sciences of the United States of America, 1939. **25**(11): p. 577.

30. Konstantinou, I.K. and T.A. Albanis, *TiO2-assisted photocatalytic degradation of azo dyes in aqueous solution: kinetic and mechanistic investigations: a review.* Applied Catalysis B: Environmental, 2004. **49**(1): p. 1-14.

31. Min, M., et al., *Micro-nano structure poly (ether sulfones)/poly (ethyleneimine) nanofibrous affinity membranes for adsorption of anionic dyes and heavy metal ions in aqueous solution.* Chemical engineering journal, 2012. **197**: p. 88-100.

32. Chen, Q., et al., *Precipitation of heavy metals from wastewater using simulated flue gas: sequent additions of fly ash, lime and carbon dioxide.* Water research, 2009. **43**(10): p. 2605-2614.

33. Razali, M., et al., *Sustainable wastewater treatment and recycling in membrane manufacturing.* Green Chemistry, 2015. **17**(12): p. 5196-5205.

34. Teh, C.Y., et al., *Recent advancement of coagulation–flocculation and its application in wastewater treatment.* Industrial & Engineering Chemistry Research, 2016. **55**(16): p. 4363-4389.

35. Pal, S., et al., *Modified guar gum/SiO 2: development and application of a novel hybrid nanocomposite as a flocculant for the treatment of wastewater.* Environmental Science: Water Research & Technology, 2015. **1**(1): p. 84-95.

36. Dąbrowski, A., et al., *Selective removal of the heavy metal ions from waters and industrial wastewaters by ion-exchange method.* Chemosphere, 2004. **56**(2): p. 91-106.

37.   Ismail, M., et al., *Green synthesis of zerovalent copper nanoparticles for efficient reduction of toxic azo dyes Congo red and methyl orange.* Green Processing and Synthesis, 2019. **8**(1): p. 135-143.

38.   Wang, J. and H. Gu, *Novel metal nanomaterials and their catalytic applications.* Molecules, 2015. **20**(9): p. 17070-17092.

39.   Yang, J., et al., *Nickel nanoparticle–chitosan-reduced graphene oxide-modified screen-printed electrodes for enzyme-free glucose sensing in portable microfluidic devices.* Biosensors and Bioelectronics, 2013. **47**: p. 530-538.

40.   Khan, A., et al., *A chemical reduction approach to the synthesis of copper nanoparticles.* International Nano Letters, 2016. **6**(1): p. 21-26.

41.   Wang, P., et al., *Application of Au based nanomaterials in analytical science.* Nano Today, 2017. **12**: p. 64-97.

42.   Kamal, T., S.B. Khan, and A.M. Asiri, *Synthesis of zero-valent Cu nanoparticles in the chitosan coating layer on cellulose microfibers: evaluation of azo dyes catalytic reduction.* Cellulose, 2016. **23**(3): p. 1911-1923.

43.   Liu, P., et al., *Nanocelluloses and their phosphorylated derivatives for selective adsorption of Ag+, Cu2+ and Fe3+ from industrial effluents.* Journal of hazardous materials, 2015. **294**: p. 177-185.

44.   Yu, X., et al., *Adsorption of heavy metal ions from aqueous solution by carboxylated cellulose nanocrystals.* Journal of Environmental Sciences, 2013. **25**(5): p. 933-943.

45.   Sehaqui, H., et al., *Enhancing adsorption of heavy metal ions onto biobased nanofibers from waste pulp residues for application in wastewater treatment.* Cellulose, 2014. **21**(4): p. 2831-2844.

46.   Peng, S., et al., *Nanoporous magnetic cellulose–chitosan composite microspheres: preparation, characterization, and application for Cu (II) adsorption.* Industrial & Engineering Chemistry Research, 2014. **53**(6): p. 2106-2113.

47.   Kenawy, I., et al., *Adsorption of Cu (II), Cd (II), Hg (II), Pb (II) and Zn (II) from aqueous single metal solutions by guanyl-modified cellulose.* International journal of biological macromolecules, 2018. **107**: p. 1538-1549.

48.   Dong, C., et al., *Efficient and selective adsorption of multi-metal ions using sulfonated cellulose as adsorbent.* Carbohydrate polymers, 2016. **151**: p. 230-236.

49. Repo, E., et al., *Adsorption of Co (II) and Ni (II) by EDTA-and/or DTPA-modified chitosan: kinetic and equilibrium modeling.* Chemical Engineering Journal, 2010. **161**(1-2): p. 73-82.

50. Saravanan, R. and L. Ravikumar, *The use of new chemically modified cellulose for heavy metal ion adsorption and antimicrobial activities.* Journal of water resource and protection, 2015. **7**(06): p. 530.

51. Sun, X., et al., *Chitosan (chitin)/cellulose composite biosorbents prepared using ionic liquid for heavy metal ions adsorption.* AIChE journal, 2009. **55**(8): p. 2062-2069.

52. Kamaruzaman, S., et al., *Removal of Cu (II) and Cd (II) ions from environmental water samples by using cellulose acetate membrane.* J Environ Anal Chem, 2017. **4**(220): p. 2380-2391.1000220.

53. Astrini, N., L. Anah, and H.R. Haryadi. *Adsorption of heavy metal ion from aqueous solution by using cellulose based hydrogel composite.* in *Macromolecular symposia.* 2015. Wiley Online Library.

54. Xiao, M. and J. Hu, *Cellulose/chitosan composites prepared in ethylene diamine/potassium thiocyanate for adsorption of heavy metal ions.* Cellulose, 2017. **24**(6): p. 2545-2557.

55. Li, N. and R. Bai, *Copper adsorption on chitosan–cellulose hydrogel beads: behaviors and mechanisms.* Separation and purification technology, 2005. **42**(3): p. 237-247.

56. Zhang, G., et al., *Dyes adsorption using a synthetic carboxymethyl cellulose-acrylic acid adsorbent.* Journal of Environmental Sciences, 2014. **26**(5): p. 1203-1211.

57. Bakhsh, E.M., et al., *Performance of cellulose acetate-ferric oxide nanocomposite supported metal catalysts toward the reduction of environmental pollutants.* International journal of biological macromolecules, 2018. **107**: p. 668-677.

58. Wang, F., et al., *Single and binary adsorption of heavy metal ions from aqueous solutions using sugarcane cellulose-based adsorbent.* Bioresource technology, 2017. **241**: p. 482-490.

59. Etim, U., S. Umoren, and U. Eduok, *Coconut coir dust as a low cost adsorbent for the removal of cationic dye from aqueous solution.* Journal of Saudi Chemical Society, 2016. **20**: p. S67-S76.

60. Senturk, H.B., D. Ozdes, and C. Duran, *Biosorption of Rhodamine 6G from aqueous solutions onto almond shell (Prunus dulcis) as a low cost biosorbent.* Desalination, 2010. **252**(1-3): p. 81-87.

61. Boumediene¹, M., et al., *Characterization of two cellulosic waste materials (orange and almond peels) and their use for the removal of methylene blue from aqueous solutions.* Maderas. Ciencia y tecnología, 2015. **17**(1): p. 69-84.

62. Witek-Krowiak, A., R.G. Szafran, and S. Modelski, *Biosorption of heavy metals from aqueous solutions onto peanut shell as a low-cost biosorbent.* Desalination, 2011. **265**(1-3): p. 126-134.

63. Nasernejad, B., et al., *Camparison for biosorption modeling of heavy metals (Cr (III), Cu (II), Zn (II)) adsorption from wastewater by carrot residues.* Process Biochemistry, 2005. **40**(3-4): p. 1319-1322.

64. Hajeeth, T., T. Gomathi, and P. Sudha. *Adsorption of copper (Ii) and nickel (Ii) ions from metal solution using graft copolymer of cellulose extracted from the sisal fiber with acrylonitrile monomer.* in *International Conference on Advanced Nanomaterials & Emerging Engineering Technologies.* 2013. IEEE.

65. Zhang, C., et al., *The removal of heavy metal ions from aqueous solutions by amine functionalized cellulose pretreated with microwave-H 2 O 2.* RSC Advances, 2017. **7**(54): p. 34182-34191.

66. Sun, X., et al., *Amino-functionalized magnetic cellulose nanocomposite as adsorbent for removal of Cr (VI): synthesis and adsorption studies.* Chemical Engineering Journal, 2014. **241**: p. 175-183.

67. Wang, L. and J. Li, *Adsorption of CI Reactive Red 228 dye from aqueous solution by modified cellulose from flax shive: Kinetics, equilibrium, and thermodynamics.* Industrial Crops and Products, 2013. **42**: p. 153-158.

68. Silva, L.S., et al., *Dye anionic sorption in aqueous solution onto a cellulose surface chemically modified with aminoethanethiol.* Chemical Engineering Journal, 2013. **218**: p. 89-98.

69. Silva, L.S., et al., *Potential of amino-functionalized cellulose as an alternative sorbent intended to remove anionic dyes from aqueous solutions.* International journal of biological macromolecules, 2018. **116**: p. 1282-1295.

70. Dragan, E.S., A.I. Cocarta, and M.V. Dinu, *Facile fabrication of chitosan/poly (vinyl amine) composite beads with enhanced sorption of Cu2+. Equilibrium, kinetics, and thermodynamics.* Chemical Engineering Journal, 2014. **255**: p. 659-669.

71. Li, X., et al., *Studies of heavy metal ion adsorption on Chitosan/Sulfydryl-functionalized graphene oxide composites.* Journal of colloid and interface science, 2015. **448**: p. 389-397.

72. Negm, N.A., et al., *Treatment of industrial wastewater containing copper and cobalt ions using modified chitosan.* Journal of Industrial and Engineering Chemistry, 2015. **21**: p. 526-534.

73. Ngah, W.W., et al., *Comparative study on adsorption and desorption of Cu (II) ions by three types of chitosan–zeolite composites.* Chemical Engineering Journal, 2013. **223**: p. 231-238.

74. Ali, M.E., *Synthesis and adsorption properties of chitosan-CDTA-GO nanocomposite for removal of hexavalent chromium from aqueous solutions.* Arabian Journal of Chemistry, 2018. **11**(7): p. 1107-1116.

75. Haider, S., et al., *Natural polymers supported copper nanoparticles for pollutants degradation.* Applied Surface Science, 2016. **387**: p. 1154-1161.

76. Li, P., et al., *Enhanced decolorization of methyl orange using zero-valent copper nanoparticles under assistance of hydrodynamic cavitation.* Ultrasonics sonochemistry, 2015. **22**: p. 132-138.

77. Ali, N., et al., *Chitosan-coated cotton cloth supported copper nanoparticles for toxic dye reduction.* International journal of biological macromolecules, 2018. **111**: p. 832-838.

78. Kamal, T., et al., *Dye adsorption and bactericidal properties of TiO2/chitosan coating layer.* Carbohydrate polymers, 2016. **148**: p. 153-160.

79. Ali, F., et al., *Chitosan coated cotton cloth supported zero-valent nanoparticles: Simple but economically viable, efficient and easily retrievable catalysts.* Scientific reports, 2017. **7**(1): p. 16957.

80. Khan, S.A., et al., *A facile synthesis of CuAg nanoparticles on highly porous ZnO/carbon black-cellulose acetate sheets for nitroarene and azo dyes reduction/degradation.* International journal of biological macromolecules, 2019. **130**: p. 288-299.

81. Khan, S.A., et al., *Antibacterial nanocomposites based on chitosan/Co-MCM as a selective and efficient adsorbent for organic dyes.* International journal of biological macromolecules, 2016. **91**: p. 744-751.

82. Xu, Y., et al., *Influence of HNO3/H3PO4–NaNO2 mediated oxidation on the structure and properties of cellulose fibers.* Carbohydrate polymers, 2014. **111**: p. 955-963.

83. Kumar, V. and T. Yang, *HNO3/H3PO4–NaNO2 mediated oxidation of cellulose—preparation and characterization of bioabsorbable oxidized celluloses in high yields and with different levels of oxidation.* Carbohydrate Polymers, 2002. **48**(4): p. 403-412.

84. Rahn, K., et al., *Homogeneous synthesis of cellulose p-toluenesulfonates in N, N-dimethylacetamide/LiCl solvent system.* Die Angewandte Makromolekulare Chemie: Applied Macromolecular Chemistry and Physics, 1996. **238**(1): p. 143-163.

85. Liu, C. and H. Baumann, *Exclusive and complete introduction of amino groups and their N-sulfo and N-carboxymethyl groups into the 6-position of cellulose without the use of protecting groups.* Carbohydrate research, 2002. **337**(14): p. 1297-1307.

86. Fifield, F.W., *Principles and practice of analytical chemistry*. 2000: Blackwell science ltd.

87. Fadeeva, V., V. Tikhova, and O. Nikulicheva, *Elemental analysis of organic compounds with the use of automated CHNS analyzers.* Journal of analytical chemistry, 2008. **63**(11): p. 1094-1106.

88. Dutrow, B. and C. Clark, *X-ray Powder Diffraction (XRD), Geochemical Instrumentation and Analysis.* Integrating Research and Education, 2016.

89. Jaffé, H.H. and M. Orchin, *Theory and applications of ultraviolet spectroscopy.* 1962.